

Likelihood-based Modeling of Covariate-Specific Time-Dependent ROC Curves

Ainesh Sewak^{ID}
Universität Bern

Vanda Inácio^{ID}
University of Edinburgh

Joanne Wuu^{ID}
University of Miami

Michael Benatar^{ID}
University of Miami

Torsten Hothorn^{ID}
Universität Zürich

Abstract

Identifying reliable biomarkers for predicting clinical events in longitudinal studies is important for accurate disease prognosis and for guiding development of new treatments. However, prognostic studies are often observational, making it difficult to account for patient heterogeneity. In amyotrophic lateral sclerosis (ALS), factors such as age, site of onset and genetic status influence both survival and biomarker levels, yet their impact on the prognostic accuracy of biomarkers over time remains unclear. While time-dependent receiver operating characteristic methods have been developed to handle censored time-to-event outcomes, most do not adjust for covariates. To address this, we propose the nonparanormal prognostic biomarker framework, which models the joint distribution of the biomarker and event time while accounting for covariates. This allows estimation of covariate-specific time-dependent ROC curves and related summary measures. We apply the NPB framework to evaluate serum neurofilament light as a prognostic biomarker in ALS, showing that its accuracy varies over time and with patient characteristics. By capturing these covariate-specific effects, the NPB framework supports more targeted risk stratification and can potentially improve the design of clinical trials for new ALS treatments.

Keywords: time-dependent ROC analysis, covariates, prognostic biomarkers, amyotrophic lateral sclerosis, censoring.

1. Introduction

Prognostic biomarkers are essential tools for predicting clinical events. They can enable more effective patient stratification and improved design of clinical trials. As the discovery of new biomarkers accelerates, so too does the need for methods to evaluate their predictive accuracy, particularly in the presence of patient heterogeneity.

Two key considerations in prognostic biomarker evaluation is that a marker's accuracy may vary over time and across subgroups defined by patient-level covariates. Understanding these is important for assessing the biomarker's clinical utility. Unlike diagnostic studies, where disease status and biomarkers are measured concurrently, prognostic studies evaluate a baseline biomarker's ability to predict future outcomes, often subject to right- or interval-censoring.

Unlike randomized trials, prognostic biomarker studies are typically observational, meaning treatment or exposure groups are not assigned at random (Freidlin *et al.* 2010). As a result, covariate imbalance and confounding are common, making it difficult to disentangle the prognostic value of the biomarker from that of patient characteristics. This challenge is particularly relevant in diseases like amyotrophic lateral sclerosis (ALS), where age, disease onset site and genetic status can influence both survival and biomarker levels.

The most common approach to handle this in medical research is to use the hazard ratio from a proportional hazards model as a summary of prognostic performance. However, association measures such as hazard ratios do not directly quantify the accuracy of a biomarker to discriminate patients at higher risk of experiencing the event (Pepe *et al.* 2004; Bansal and Heagerty 2019). Moreover, the proportional hazards assumption is frequently violated in practice, potentially leading to misleading inference (Stensrud and Hernà 2025).

To address these limitations, time-dependent extensions of classical accuracy metrics such as sensitivity, specificity, the receiver operating characteristic (ROC) curve and the area under the curve (AUC) have been developed (Slate and Turnbull 2000; Heagerty and Zheng 2005; Cai *et al.* 2006). In this work, we focus on the cumulative sensitivity and dynamic specificity framework, which is widely adopted in clinical research (Lambert and Chevret 2016). A large body of work exists on time-dependent ROC analysis, including nonparametric and semiparametric estimators. For a review, see Blanche *et al.* (2013b); Kamarudin *et al.* (2017).

However, comparatively fewer methods account for covariates when assessing prognostic accuracy, despite growing evidence that ignoring patient heterogeneity can bias ROC-based estimates (Janes and Pepe 2008). Three main classes of methods have been proposed for covariate adjustment in time-dependent ROC analysis: (1) model-based approaches that rely on proportional hazards models for event times given the biomarker and covariates (Song and Zhou 2008; Li and Ning 2015), which are sensitive to the proportional hazards model assumption; (2) fully nonparametric methods using kernel smoothing (Rodríguez-Álvarez *et al.* 2016), which are limited to a single continuous covariate and exhibit high variance; and (3) more recent strategies based on covariate standardization or marginalization (Le Borgne *et al.* 2018; Dey *et al.* 2023; Jiang *et al.* 2024), which provide population-averaged rather than covariate-specific accuracy estimates.

In this paper, we propose a modeling framework for covariate-specific, time-dependent ROC analysis that addresses several key limitations of existing methods. Our approach combines semiparametric marginal transformation models for the biomarker and event times, which incorporate covariate effects and are linked via a copula to capture their joint dependence. The model is efficiently parameterized, making it well-suited for small to moderate sample sizes that are common in prognostic biomarker studies. Unlike fully nonparametric approaches, our framework is more efficient, accommodates multiple covariates and allows for both covariate-specific and population-averaged accuracy estimates. A major advantage is its ability to handle both right- and interval-censored outcomes within a unified likelihood framework, avoiding the need for separate estimators (Beyene and El Ghouch 2020, 2022). While the Gaussian copula imposes a structured form of dependence, it enables tractable estimation and facilitates meaningful extensions, such as modeling detection limits for biomarkers and covariate-dependent censoring, that are difficult to implement using kernel-based or fully nonparametric methods.

The layout of the paper is as follows. We begin with our motivation in Section 2, using

biomarker and event time data from a longitudinal study on amyotrophic lateral sclerosis (ALS). Section 3 introduces key concepts, including sensitivity, specificity and the covariate-specific cumulative-dynamic ROC curve. In Section 4, we present the technical details of our model, including parameterization and inference. In Section 5, we explore potential extensions of our approach and detail a technique for model assessment. Section 6 provides results from a simulation study with a detailed comparison to existing methods. In Section 7, we apply our method to the ALS study data. We offer concluding remarks in Section 8.

2. Prognostic biomarkers in ALS

ALS is a progressive neurodegenerative disease that causes degeneration of nerve cells, leading to muscle weakness, paralysis and respiratory failure. With a median survival duration of 20 to 48 months after symptom onset, ALS currently has no cure and available treatments primarily aim to manage the symptoms and slow disease progression (Feldman *et al.* 2022). Identifying reliable prognostic biomarkers for ALS are essential for improving clinical trial design (Kiernan *et al.* 2021; Benatar *et al.* 2024). Biomarkers may be utilized in trial designs to stratify patients into homogeneous subgroups, serve as eligibility criteria to define appropriate study populations and act as baseline covariates to adjust for patient heterogeneity. Together, these applications reduce sample size requirements, enable more cost-effective studies, and accelerate the development of effective treatments (Taga and Maragakis 2018).

2.1. Longitudinal ALS cohort

The methods developed in this article are motivated by a prospective longitudinal study on the prognostic utility of neurofilament biomarkers for amyotrophic lateral sclerosis (ALS), as described by Benatar *et al.* (2020). One of the outcomes of the study was survival duration, defined as the time from the baseline visit to either permanent assisted ventilation, tracheostomy, or death. Patients who did not experience any of these events during the follow-up period were right-censored. Our study analyzed a subset of 260 patients enrolled across multiple clinical sites through the Clinical Research in ALS and Related Disorders for Therapeutic Development (CReATe) Consortium's Phenotype-Genotype-Biomarker study (registered at clinicaltrials.gov: NCT02327845), representing the data available for biomarker analysis at the time of a prior publication (Benatar *et al.* 2020). Patients included in the present study comprised 229 patients with ALS, 11 with progressive muscle atrophy (PMA), and 20 with primary lateral sclerosis. To discover and validate biomarkers, all patients underwent systematic follow-ups with standardized clinical evaluations and provided biological samples every 3 to 6 months. For our analysis, we included patients with ALS or PMA. After excluding 12 patients with missing values in one or more covariates, the final sample comprised $N = 218$ patients.

The biomarker of interest in our study is serum neurofilament light (NfL) concentration. Baseline serum NfL concentration has been shown to differentiate ALS patients from healthy controls and is associated with both survival outcomes and disease progression in ALS (Lu *et al.* 2015; Benatar *et al.* 2024). Figure 1 illustrates the observed relationship between baseline NfL and survival duration in the present study, showing that higher baseline NfL levels are generally associated with shorter survival. However, this association is not strictly linear and any evaluation of prognostic accuracy must account for the right-censored data in

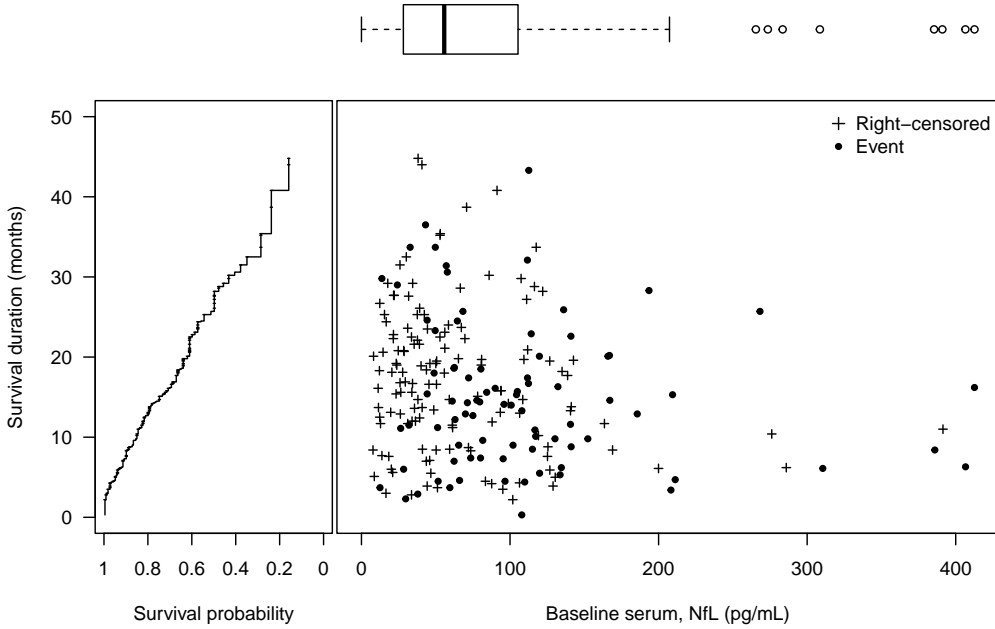


Figure 1: Scatter plot of the observed baseline serum neurofilament light (NfL) concentration (pg/mL) and survival duration (in months since baseline). Right censored subjects are indicated with “+” and subjects who reached the endpoint are marked by “•”.

the study. Furthermore, the prognostic accuracy of NfL may depend on the time horizon of prediction and could be influenced by patient characteristics.

2.2. Challenges in assessing prognostic accuracy

Evaluating the prognostic accuracy of ALS biomarkers in observational studies is challenging because of the risk of confounding. Confounding arises when covariates such as age are associated with both biomarker levels and disease prognosis. For example, older patients tend to have elevated NfL levels and face an increased risk of ALS-related mortality, potentially distorting the accuracy of NfL as a prognostic marker. While factors such as aging and site of onset are known to be associated with NfL levels, their impact on NfL’s prognostic accuracy across different time horizons remains unclear (Koini *et al.* 2021; Benatar *et al.* 2023).

Stratifying by covariates can help address confounding, but this approach is limited to a small number of categorical covariates and often results in small sample sizes in each group, limiting the ability to draw statistically efficient conclusions. In ALS, where large datasets are scarce, proportional hazards models are commonly used to estimate an overall hazard ratio. Such regression models account for confounding and can give an indication of the prognostic utility of NfL by quantifying its association with survival duration. However, they do not fully capture how NfL’s prognostic accuracy changes across different time horizons. Additionally, these models assume that the relationship between NfL, covariates, and survival duration remains proportional over time. This is a condition that may not hold in a progressive disease like ALS, where risk dynamics evolve (Stensrud and Hernà 2025).

To address these limitations, covariate-specific sensitivity and specificity can be used to assess a biomarker’s ability to predict survival. These measures form the foundation of ROC analysis and provide a framework for evaluating prognostic accuracy across different time horizons.

3. Evaluation of prognostic biomarkers

We first provide a brief overview of evaluating the accuracy of a continuous biomarker Y in predicting a time-constant binary outcome D , where $D = 0$ represents “controls” and $D = 1$ represents “cases”. Assuming higher values of Y are more indicative of disease, a threshold $c \in \mathbb{R}$ can be used to classify subjects as cases if their biomarker value exceeds c , and as controls otherwise. Sensitivity is the correct classification probability for cases, defined as $\text{Se}(c) = \mathbb{P}(Y > c \mid D = 1)$, while specificity represents the correct classification probability for controls, $\text{Sp}(c) = \mathbb{P}(Y < c \mid D = 0)$. For any given biomarker, there is a trade-off between sensitivity and specificity, as increasing one decreases the other. This trade-off is determined by the choice of c . The ROC curve is a graphical tool that plots sensitivity against $1 - \text{specificity}$ for all possible threshold values of c and provides a measure of the biomarker’s diagnostic accuracy.

Most diseases do not present binary outcomes. Instead, they often involve longitudinal outcomes, such as survival duration for ALS patients. To accommodate this, various extensions have been developed to measure time-dependent sensitivity and specificity (Heagerty and Zheng 2005). We focus on the cumulative sensitivity and dynamic specificity because our interest lies in evaluating the accuracy of prognostic ALS biomarkers at specific time points. Additionally, both the biomarker and survival duration might depend on a set of covariates $\mathbf{X} = (X_1, \dots, X_p)$ such as age, sex, genetic factors and disease progression which need to be taken into account.

For the event time T , we define the covariate-specific cumulative sensitivity and dynamic specificity as

$$\begin{aligned}\text{Se}_t^{\mathbb{C}}(c \mid \mathbf{x}) &= \mathbb{P}(Y > c \mid T \leq t, \mathbf{X} = \mathbf{x}) \\ \text{Sp}_t^{\mathbb{D}}(c \mid \mathbf{x}) &= \mathbb{P}(Y \leq c \mid T > t, \mathbf{X} = \mathbf{x}).\end{aligned}$$

In this context, *cumulative* sensitivity considers any subject who experiences the event before a time point of interest t as a case (i.e., $T \leq t$, or conceptually, $D(t) = I(T \leq t) = 1$), while *dynamic* specificity defines a control as any subject who remains event-free at time t (i.e., $T > t$, or $D(t) = 0$). For a fixed time t , the entire population is thus classified into cases (those who have experienced the event) and controls (those still at risk).

These definitions lead to the *cumulative-dynamic* ROC curve, which assesses the biomarker’s prognostic accuracy for a given time horizon. This enables evaluation of how effectively a baseline marker can differentiate between subjects who will experience the event of interest and those who will not within a specified follow-up interval. Each time horizon of interest may yield a different accuracy, reflecting the dynamic nature of time-to-event data. The covariate-specific cumulative-dynamic ROC curve is given by

$$\text{ROC}_t^{\mathbb{C}/\mathbb{D}}(p \mid \mathbf{x}) = \text{Se}_t^{\mathbb{C}} \left([1 - \text{Sp}_t^{\mathbb{D}}]^{-1}(p \mid \mathbf{x}) \mid \mathbf{x} \right), \text{ for } p \in [0, 1],$$

where the function $[1 - \text{Sp}_t^{\mathbb{D}}]^{-1}(p) = \inf \{c \in \mathbb{R} : 1 - \text{Sp}_t^{\mathbb{D}}(c) \leq p\}$ exists. These definitions

allow for assessing a biomarker's prognostic accuracy for subjects with shared characteristics $\mathbf{X} = \mathbf{x}$.

The area under the cumulative-dynamic ROC curve (AUC) is the most widely used summary measure of the ROC curve and represents the probability that a subject with a higher biomarker value experienced the event earlier. The corresponding covariate-specific time-dependent AUC is defined as

$$\text{AUC}_t(\mathbf{x}) = \int_0^1 \text{ROC}_t^{\mathbb{C}/\mathbb{D}}(p \mid \mathbf{x}) dp = \mathbb{P}(Y_i > Y_j \mid T_i \leq t, T_j > t, \mathbf{X}_i = \mathbf{X}_j = \mathbf{x})$$

for two distinct subjects i and j . Other measures, such as the Youden Index and optimal cut-off values, can also be derived once the ROC curve is obtained. Although this paper focuses on the cumulative-dynamic ROC curve, the methods discussed can estimate other forms of time-dependent ROC curves in the same statistical framework as well. Additional details for these approaches are provided in Supplementary Material A.

4. The nonparanormal prognostic biomarker model

We propose the nonparanormal prognostic biomarker (NPB) model as a flexible framework for covariate-specific, time-dependent ROC analysis. The NPB model comprises two main components: (1) a joint model that captures the dependence between the biomarker and event time, and (2) marginal transformation models for each variable that incorporate covariate effects. The name “nonparanormal” reflects the structure of the likelihood, which combines these two components into a unified framework.

Using Bayes' theorem, for a fixed time t , the cumulative sensitivity can be expressed as

$$\text{Se}_t^{\mathbb{C}}(c \mid \mathbf{x}) = \frac{\mathbb{P}(Y > c, T \leq t \mid \mathbf{X} = \mathbf{x})}{\mathbb{P}(T \leq t \mid \mathbf{X} = \mathbf{x})} = \frac{F_T(t \mid \mathbf{x}) - F_{Y,T}(c, t \mid \mathbf{x})}{F_T(t \mid \mathbf{x})},$$

where $F_T(t \mid \mathbf{x})$ is the marginal cumulative distribution function (CDF) of the event time conditioned on the covariates \mathbf{x} and $F_{Y,T}(y, t \mid \mathbf{x})$ is the joint conditional CDF of the biomarker and event time. Similarly, the dynamic specificity at time t is given by

$$\text{Sp}_t^{\mathbb{D}}(c \mid \mathbf{x}) = \frac{\mathbb{P}(Y \leq c, T > t \mid \mathbf{X} = \mathbf{x})}{\mathbb{P}(T > t \mid \mathbf{X} = \mathbf{x})} = \frac{F_Y(c \mid \mathbf{x}) - F_{Y,T}(c, t \mid \mathbf{x})}{1 - F_T(t \mid \mathbf{x})},$$

where $F_Y(c \mid \mathbf{x})$ is the marginal CDF of the biomarker. Notice that if the joint conditional distribution of (Y, T) given $\mathbf{X} = \mathbf{x}$ is known, all terms in these expressions can be derived. Further, we can calculate cumulative sensitivity and dynamic specificity for a range of cut-off points $c \in \mathbb{R}$ and plot the corresponding ROC curve for a specific time t conditional on covariate values \mathbf{x} . The time-dependent covariate-specific AUC can then be obtained by numerically integrating the corresponding ROC curve.

In this paper, we focus on flexibly modeling the joint conditional distribution $F_{Y,T}(y, t \mid \mathbf{x})$ of the biomarker and event time given $\mathbf{X} = \mathbf{x}$. This approach allows us to calculate model-based covariate-specific cumulative sensitivity, dynamic specificity, and construct time-dependent covariate-specific ROC curves and corresponding summary metrics such as $\text{AUC}_t(\mathbf{x})$. Next, we detail the components of the model followed by a likelihood-based estimation approach that can accommodate both right and interval censoring schemes.

4.1. Joint model specification

Semiparametric regression models that incorporate covariate effects are well-established for modeling either the distribution of a biomarker (Pepe 1997) or the distribution of event times (Cox 1972), both of which may be subject to censoring. However, jointly modeling the conditional distribution of the biomarker and the event time poses additional challenges, particularly in capturing their dependence structure in a way that accommodates covariates and censoring.

To address this, we adopt a nonparanormal copula model (Liu *et al.* 2009), which links semiparametric marginal models for the biomarker and event time via a Gaussian copula. Specifically, we model the conditional joint distribution of $(Y, T) | \mathbf{X} = \mathbf{x}$ as

$$\begin{aligned} F_{Y,T}(y, t | \mathbf{x}) &= \mathbb{P}(Y \leq y, T \leq t | \mathbf{X} = \mathbf{x}) \\ &= C_\rho(F_Y(y | \mathbf{x}), F_T(t | \mathbf{x})) \\ &= \Phi_\rho(\Phi^{-1}(F_Y(y | \mathbf{x})), \Phi^{-1}(F_T(t | \mathbf{x}))) \end{aligned}$$

where Φ denotes the CDF of a standard normal distribution and $\Phi_\rho(z_1, z_2)$ is the CDF of the bivariate standard normal distribution with correlation parameter $\rho \in [-1, 1]$. The copula C_ρ captures the dependence structure between the biomarker and event time, leaving their marginal distributions unspecified. We define monotonically nondecreasing marginal transformation functions as

$$h_Y(y | \mathbf{x}) = \Phi^{-1}(F_Y(y | \mathbf{x})) \text{ and } h_T(t | \mathbf{x}) = \Phi^{-1}(F_T(t | \mathbf{x})),$$

which map the conditional marginals to the standard normal scale. Under this model, the latent variables follow a bivariate normal distribution

$$\mathbf{Z} = (h_Y(Y | \mathbf{x}), h_T(T | \mathbf{x}))^\top \sim N_2\left(\mathbf{0}, \begin{pmatrix} 1 & \rho \\ \rho & 1 \end{pmatrix}\right).$$

This transformation simplifies inference while allowing flexible specification of each marginal via semiparametric transformation models. In practice, the marginal models for Y and T may depend on different covariates. We assume the same covariate set for notational simplicity.

While we focus on the Gaussian copula due to its computational tractability, particularly the availability of closed-form likelihood and score functions, our framework can accommodate other parametric copulas if needed. In Section 5, we also describe how to extend the model to allow for covariate-specific correlation, which relaxes the assumption of constant dependence across the population.

4.2. Marginal model parameterization

We model the marginal distributions semiparametrically using probit linear transformation models

$$F_Y(y | \mathbf{x}) = \Phi\left(h_Y(y) - \mathbf{x}^\top \boldsymbol{\beta}_Y\right) \text{ and } F_T(t | \mathbf{x}) = \Phi\left(h_T(t) - \mathbf{x}^\top \boldsymbol{\beta}_T\right),$$

where h_Y and h_T are baseline transformation functions that map the biomarker Y and event time T to the latent normal scale, and $\boldsymbol{\beta}_Y$ and $\boldsymbol{\beta}_T$ are the respective linear covariate effects. Under this specification, the joint conditional CDF of $(Y, T) | \mathbf{X} = \mathbf{x}$ is given by

$$F_{Y,T}(y, t | \mathbf{x}) = \Phi_\rho\left(h_Y(y) - \mathbf{x}^\top \boldsymbol{\beta}_Y, h_T(t) - \mathbf{x}^\top \boldsymbol{\beta}_T\right), \quad (1)$$

and the corresponding joint conditional density function is

$$f_{Y,T}(y, t | \mathbf{x}) = \phi_\rho \left(h_Y(y) - \mathbf{x}^\top \boldsymbol{\beta}_Y, h_T(t) - \mathbf{x}^\top \boldsymbol{\beta}_T \right) h'_Y(y) h'_T(t). \quad (2)$$

We adopt the probit link here for notational clarity, but other choices are compatible within this framework. For instance, the transformation functions can be specified to correspond to proportional hazards or proportional odds models. These alternatives are discussed in detail in Section 5.

We model the baseline transformation function for the biomarker as a smooth, monotonically nondecreasing function of y , defined as

$$h_Y(y | \boldsymbol{\vartheta}_Y) = \mathbf{b}(y)^\top \boldsymbol{\vartheta}_Y = \sum_{m=0}^M \vartheta_{Y,m} b_m(y),$$

where $\mathbf{b}(y) = (b_0(y), \dots, b_M(y))^\top$ is a vector of $M + 1$ basis functions with coefficients $\boldsymbol{\vartheta}_Y \in \mathbb{R}^{M+1}$ (Hothorn *et al.* 2018). We use Bernstein polynomials as the basis functions, as they provide a flexible yet structured way to approximate any continuous function on a bounded interval (Farouki 2012). The degree M controls the smoothness of the transformation; for example, $M = 1$ corresponds to a linear transformation, while in practice we find that $M = 6$ is sufficient for capturing most empirical biomarker distributions (Sewak and Hothorn 2023).

To ensure that h_Y is nondecreasing, we impose monotonicity constraints on the coefficients $\vartheta_{Y,m} \leq \vartheta_{Y,m+1}$ for $m = 0, \dots, M - 1$. The Bernstein basis polynomial of order M on the interval $[l, u]$ is given by

$$b_m(y) = \binom{M}{m} \tilde{y}^m (1 - \tilde{y})^{M-m}, \quad m = 0, \dots, M,$$

where the observations are rescaled to the unit interval via $\tilde{y} = \frac{y-l}{u-l}$. The baseline transformation function for survival time is parameterized in the same manner, with its own coefficient vector denoted by $\boldsymbol{\vartheta}_T$.

4.3. Likelihood inference

The complete set of parameters for our model is denoted as $\boldsymbol{\theta} = (\boldsymbol{\vartheta}_Y^\top, \boldsymbol{\vartheta}_T^\top, \boldsymbol{\beta}_Y^\top, \boldsymbol{\beta}_T^\top, \rho)^\top$. The likelihood in our model corresponds to the “mixed nonparanormal likelihood” with smooth parameterization of the marginal transformation functions (Hothorn 2024b). This mixed likelihood structure accommodates both censored and continuous responses. It results in a “flow nonparanormal likelihood” for continuous variables and an interval-censored likelihood defined by the conditional distribution of censored event time observations. In the bivariate case considered here, our model accounts for two main types of observations: exact and interval-censored. Let N_e denote the number of observations with exact event times and N_c those with interval-censored events, for a total of $N = N_e + N_c$ observations.

For exact (uncensored) observations, we observe $O_i = (y_i, t_i, \mathbf{x}_i)$ for $i = 1, \dots, N_e$. The likelihood contribution is given by the joint conditional density

$$\ell_e(\boldsymbol{\theta} | O_i) = f_{Y,T}(y_i, t_i | \mathbf{x}_i, \boldsymbol{\theta})$$

as defined in Equation 2.

For interval-censored event times, where biomarker values are observed exactly and the event time falls in a known interval (t_i, \bar{t}_i) , the observation is $O_i = (y_i, t_i, \bar{t}_i, \mathbf{x}_i)$ for $i = N_e + 1, \dots, N$. Assuming conditional independence, the likelihood contribution is

$$\ell_c(\boldsymbol{\theta} | O_i) = \int_{h_T(t_i | \boldsymbol{\vartheta}_T)}^{h_T(\bar{t}_i | \boldsymbol{\vartheta}_T)} \phi_\rho \left(h_Y(y_i | \boldsymbol{\vartheta}_Y) - \mathbf{x}_i^\top \boldsymbol{\beta}_Y, z_T - \mathbf{x}_i^\top \boldsymbol{\beta}_T \right) h'_Y(y_i) dz_T,$$

where ϕ_ρ is the bivariate normal density with correlation ρ and the integral represents the probability mass over the censored time interval. Right-censored observations are handled as a special case of this likelihood by setting $\bar{t}_i = \infty$. The full log-likelihood is then constructed as

$$\ell(\boldsymbol{\theta} | \mathbf{O}) = \sum_{i=1}^{N_e} \log(\ell_e(\boldsymbol{\theta} | O_i)) + \sum_{i=N_e+1}^N \log(\ell_c(\boldsymbol{\theta} | O_i)),$$

where $\mathbf{O} = \{O_1, \dots, O_N\}$ denotes the complete dataset.

Maximum likelihood estimation of $\boldsymbol{\theta}$ is carried out via constrained optimization, requiring repeated evaluation of multivariate normal probabilities. These are efficiently computed using randomized quasi-Monte Carlo integration methods (Genz 1992) and implemented in the **mvtnorm** package (Hothorn 2024a). The corresponding score functions are available in closed form and described in detail elsewhere (Hothorn 2024b). A practical advantage of the proposed framework is that the estimation of the marginal distributions can be performed separately from the dependence structure. This allows for efficient and numerically stable initialization of parameters through low-dimensional, convex optimization problems, which facilitates reliable convergence when fitting the full joint model.

5. Extensions and model assessment

In this section, we outline several extensions of the NPB framework that increase its applicability in more complex settings. These include handling limits of detection in biomarker measurements, accommodating informative or non-independent censoring, modeling covariate-specific correlation structures and incorporating nonlinear covariate effects. While these features were not applied in the ALS case study, the NPB framework can support them. Importantly, all of these extensions are already implemented in the **tram** package in R. We also present a graphical model assessment strategy based on PIT transformations to evaluate model calibration.

5.1. Limit of detection in biomarkers

Biomarker measurements are often affected by random errors and limits of detection issues. Ignoring of such a data characteristic can reduce the biomarker's prognostic accuracy. Statistically, this is a form of interval censoring where measurements below the detection limit are left-censored and those above the detection limit are right-censored. In the NPB framework, the likelihood can be adjusted to account for this censoring in the biomarker data. For independent interval-censored biomarker measurements and interval-censored event times, we

observe $O_i = (\underline{y}_i, \bar{y}_i, \underline{t}_i, \bar{t}_i, \mathbf{x}_i)$ and the likelihood contribution is expressed as

$$\ell_c(\boldsymbol{\theta} | O_i) = \int_{h_Y(\underline{y}_i | \boldsymbol{\vartheta}_Y)}^{h_Y(\bar{y}_i | \boldsymbol{\vartheta}_Y)} \int_{h_T(\underline{t}_i | \boldsymbol{\vartheta}_T)}^{h_T(\bar{t}_i | \boldsymbol{\vartheta}_T)} \phi_\rho \left(z_Y - \mathbf{x}_i^\top \boldsymbol{\beta}_Y, z_T - \mathbf{x}_i^\top \boldsymbol{\beta}_T \right) dz_Y dz_T.$$

In this formulation, lower detection limits are treated as a special case where $\underline{y}_i = -\infty$ and upper detection limits are treated as $\bar{y}_i = \infty$. Inference can subsequently proceed as detailed previously and the resulting estimates would not suffer from the negative bias of ignoring the true nature of the biomarker measurement.

5.2. Dependent censoring

In the methods presented above, we assumed conditionally independent censoring. That is, once the covariates \mathbf{X} are known, the event time T and censoring time C are independent, i.e., $T \perp\!\!\!\perp C | \mathbf{X} = \mathbf{x}$. However, this assumption may not hold in practice. Event time can influence censoring time and censoring may depend on biomarker levels. For example, in ALS, elevated levels of NfL might be associated with a higher risk of death, leading to study dropout as patients become too sick for follow-up.

To address this, the NPB framework can be extended to model the joint relationship between Y , T , and C given $\mathbf{X} = \mathbf{x}$, allowing for non-independent censoring. Under certain conditions, such a model is identifiable when the marginal distributions of T and C are parametrically specified, for example, as log-normal or Weibull distributions (Czado and Van Keilegom 2023). Alternatively, the event time can be modeled semiparametrically with a Cox proportional hazards model while censoring times follow a Weibull model (Deresa and Van Keilegom 2024). From any such trivariate model, we can derive the bivariate distribution of $(Y, T) | \mathbf{X} = \mathbf{x}$ using the Gaussian copula, now parameterized by a correlation matrix rather than a single parameter. The multivariate normal distribution's properties allow us to subset the rows and columns of the correlation matrix related to Y and T , and proceed with calculating cumulative sensitivity and dynamic specificity as in the original model.

5.3. Covariate-specific correlation

In some medical conditions, the correlation between a biomarker and event time can vary based on covariates. For example, in ALS, the correlation between NfL levels and survival duration may depend on covariates such as age or disease onset site. Younger patients with limb-onset ALS might exhibit a weaker correlation between NfL and survival, whereas older patients or those with bulbar-onset ALS may show a stronger correlation due to faster disease progression.

In the NPB framework, the correlation matrix $\boldsymbol{\Sigma}$ can vary with the covariates \mathbf{x} , allowing the dependence structure between Y and T to change as a function of \mathbf{x} . For the bivariate case, the correlation between Y and T for a given set of covariates \mathbf{x} is given by

$$\rho(\mathbf{x}) = \frac{-\lambda(\mathbf{x})}{\sqrt{\lambda(\mathbf{x})^2 + 1}},$$

where $\lambda(\mathbf{x}) = \alpha + \mathbf{x}^\top \boldsymbol{\gamma}$ is one possible parameterization of the coefficient of the inverse Cholesky factor (Klein *et al.* 2022; Barratt and Boyd 2023). This extension allows the model to capture subgroup-specific relationships between the biomarker and event time.

5.4. Alternative marginal models

The assumption of probit semiparametric transformation models can also be relaxed. An alternative approach is to use a continuous odds logistic regression model for the biomarker, known for its robustness properties (Harrell 2015), alongside a proportional hazards model for the event time

$$F_Y(y \mid \mathbf{x}) = \text{expit}\left(h_Y(y) - \mathbf{x}^\top \boldsymbol{\beta}_Y\right) \text{ and } F_T(t \mid \mathbf{x}) = 1 - \exp\left(-\exp\left(h_T(t) - \mathbf{x}^\top \boldsymbol{\beta}_T\right)\right).$$

In general, any absolutely continuous cumulative distribution function with a log-concave density can be substituted for the probit link function, providing flexibility in marginal model choice.

5.5. Nonlinear covariate modeling

The linear predictor in our marginal models may be insufficient to fully capture the effects of covariates in some cases. To address this, we can incorporate covariates directly into the NPB framework by estimating the joint distribution of (Y, T, \mathbf{X}) using the parameterizations and estimation procedures described earlier (Hothorn 2024b). This aligns to the approach of Rodríguez-Álvarez *et al.* (2016) but can be extended to incorporate multiple covariates. Continuous covariates can be parameterized using any polynomial or spline basis. To generate covariate-specific time-dependent ROC curves, we can determine the conditional distribution of $(Y, T) \mid \mathbf{X} = \mathbf{x}$ from the Gaussian copula.

5.6. Model assessment

Model assessment is important for evaluating the adequacy of both the marginal distributions and the joint dependence structure. A key tool for assessing calibration is the probability integral transform (PIT) (Dawid 1984). For a continuous random variable Z with true cumulative distribution function F_Z , the transformed value $F_Z(Z)$ follows a standard uniform distribution $U(0, 1)$. We can substitute the estimated CDF \hat{F}_Z and compute $\hat{F}_Z(Z_i)$ on the observed data. If the model is correctly specified, the PIT values should approximately follow an uniform distribution. This can be assessed visually using a histogram or a quantile-quantile (QQ) plot (Gneiting *et al.* 2007). Systematic deviations from uniformity suggest miscalibration or misspecification in the modeled distribution.

The PIT can be extended to the multivariate setting via the Rosenblatt transformation (Rosenblatt 1952). For the bivariate vector of biomarker and event time (Y, T) , we define the transformed variables as

$$U_1 = F_T(T), \quad U_2 = F_{Y|T}(Y \mid T)$$

where U_1 and U_2 are independent and uniformly distributed on $[0, 1]$ if the joint model is correctly specified. In our framework, these conditional distributions are univariate Gaussian and the PIT quantities can be computed directly from the fitted model parameters. Calibration of the bivariate model can then be assessed by examining the marginal uniformity of U_1 and U_2 . Empirical deviations from uniformity provide evidence of model misspecification.

In practice, however, such multivariate PIT diagnostics have rarely been applied in the presence of censoring, as censoring complicates the transformation. When the event time T is

subject to right-censoring, the PIT value $F_T(T)$ for a censored observation is only known to lie within the interval $[F_T(T), 1]$. To address this, we use a Kaplan–Meier (KM) estimator, where PIT values for censored observations are treated as random draws from $U(F_T(T), 1)$ (Klugman and Parsa 1999). In the presence of covariates, this corresponds to using the KM estimate of $F_T(T | \mathbf{X})$.

For the conditional PIT value $F_{Y|T,\mathbf{X}}(Y | T > \underline{t}, \mathbf{X})$, the complication again arises due to censoring of the event time. When the observed data consist of $O = (y, \underline{t}, \mathbf{x})$, indicating that the event time is right-censored at \underline{t} , we estimate the conditional distribution of Y given $T > \underline{t}$ and covariates $\mathbf{X} = \mathbf{x}$ using

$$P(Y \leq y | T > \underline{t}, \mathbf{X} = \mathbf{x}) = \frac{F_{Y|\mathbf{X}}(y | \mathbf{x}) - F_{Y,T|\mathbf{X}}(y, \underline{t} | \mathbf{x})}{1 - F_{T|\mathbf{X}}(\underline{t} | \mathbf{x})}.$$

This expression enables the computation of PIT values for censored event times while appropriately conditioning on covariates. These PIT-based tools offer an approach for assessing model calibration, both in the presence and absence of censoring, and under covariate adjustment. We demonstrate their use in the application that follows in Section 7.

6. Empirical evaluation

In this section, we use simulated data to evaluate the performance of our NPB model in assessing the prognostic accuracy of biomarkers. Since most existing methods for time-dependent ROC analysis do not account for covariates, we begin by comparing these methods in the unconditional scenario, followed by a comparison when covariates are introduced. For competitor methods in the unconditional case, we considered actively maintained R packages that are hosted and systematically checked on the Comprehensive R Archive Network (CRAN), as summarized in Table 1. For a review of these methods, see Kamarudin *et al.* (2017).

Package	Methods	Reference
survivalROC	Nearest neighbor estimation (NNE), Kaplan-Meier (KM)	Heagerty <i>et al.</i> (2000)
timeROC	Inverse probability weighting (IPW)	Blanche <i>et al.</i> (2013a)
smoothROCtime	Bivariate kernel density estimation	Martínez-Camblor and Pardo-Fernández (2018)
nsROC	Cox proportional hazards model (COX), Kaplan-Meier (KM) and weighted Kaplan-Meier (WKM)	Pérez-Fernández <i>et al.</i> (2018)
cenROC	Weighted kernel smoother with (TR) and without boundary correction (UTR)	Beyene and El Ghouch (2020)
tdROC	Nonparametric weight adjustments	Li <i>et al.</i> (2018)

Table 1: R packages and methods for unconditional time-dependent ROC analysis.

We label each method using the R package name, followed by an abbreviation for the specific estimator when multiple options are available within the same package.

6.1. Data generating process

For the biomarker, we as data generating process (DGP) considered the following distributions F_Y : standard normal $N(0, 1)$, two-component normal mixture of $N(1, 1)$ and $N(4, 1.5^2)$ with equal mixture weights, and the Chi-squared with three degrees of freedom. For event time, we used the following distributions F_T : standard lognormal, Weibull with shape 1.4 and rate 2.0, and Gamma with shape 1.5 and rate 1.2. We explored all combinations of biomarker and event time distributions, with sample sizes of $N \in \{100, 500, 1000\}$ for a 1000 replications. This data generation approach is similar to that used in previous studies (Martínez-Camblor and Pardo-Fernández 2018; Yu and Hwang 2019; Beyene and Chen 2024).

We generated $\mathbf{Z} = (Z_1, Z_2)^\top$ from a standard bivariate normal distribution with correlation coefficient $\rho \in \{-0.3, -0.5\}$. The negative correlation implies that higher baseline biomarker concentrations are associated with shorter event times. To explore the range of marginal distributions, we transformed the marginals to uniform distributions $(U_1, U_2) = (\Phi(Z_1), \Phi(Z_2))$ and applied different quantile functions to obtain the desired distributions of the biomarker and event time (Y, T) . This preserves the dependence structure governed by ρ while allowing the marginal distributions to vary.

To achieve an expected censoring rate of 50%, the censoring time C can be generated independently following the same distribution as the event time. For any other censoring rate $\kappa = \mathbb{P}(T > C)$, independent realizations can be drawn from a distribution of the same form as the event time, given by $F_C(c) = \Phi(h_T(c) + a)$, where $a = \Phi^{-1}(\kappa)\sqrt{2}$ is an offset based on the definition of the AUC used to achieve the target censoring rate (Sewak and Hothorn 2023). In our study, we applied censoring rates of $\kappa \in \{0.3, 0.5\}$.

6.2. Unconditional results

We evaluated the AUC at times corresponding to the unconditional quantiles 0.1, 0.25, 0.5, and 0.75 for each estimator and biomarker distribution. Figure 3 displays the mean and standard error across the 1000 repetitions of the estimated AUC for different methods and sample sizes. The NPB method shows a small bias for small sample sizes but is generally unbiased for larger sample sizes across different time quantiles and biomarker distributions. Additionally, the NPB model demonstrates lower variability compared to other methods. In contrast, the NNE estimator from **survivalROC** exhibits bias in all scenarios. Most methods are unbiased for time quantiles below 0.5, but **smoothROCtime** and **nsROC** have some bias for higher time quantiles. The results were consistent across different event time distributions. Results for a lognormal event time distribution, a 50% censoring rate and a correlation of $\rho = -0.7$ are shown in Supplementary Figure 9.

For the ROC curve, we calculated the root integrated squared error (RISE)

$$\text{RISE} = \sqrt{\int_0^1 \left(\widehat{\text{ROC}}_t(p) - \text{ROC}_t(p) \right)^2 dp}$$

where $\widehat{\text{ROC}}_t$ is the estimated ROC curve and ROC_t is the true curve for a given time point t . Figure 3 displays the RISE distribution for the time quantile 0.5 for different biomarker and event time distributions. The NPB method achieves lowest RISE values across all setups, indicating better performance in estimating the ROC curve. Methods like **survivalROC** (NNE and KM) and **timeROC** show higher RISE values, suggesting less precise estimates. Kernel-based

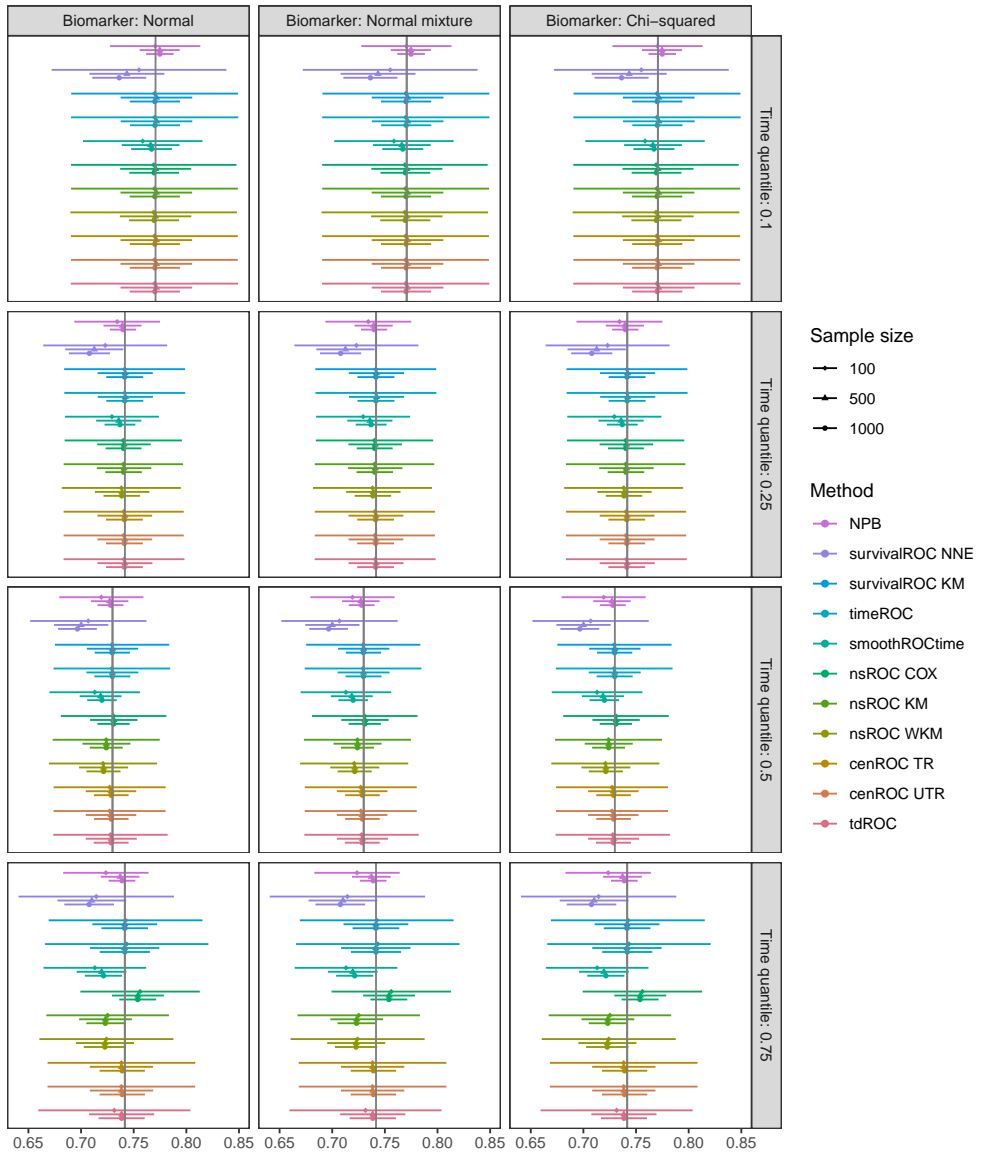


Figure 2: Mean and standard deviation of the unconditional AUC for each method with sample sizes of $N = \{100, 500, 1000\}$, Weibull event time distribution, 30% censoring rate and a correlation of $\rho = -0.5$ between transformed biomarker and event time distributions. The evaluation is across different biomarker distributions (Normal, Normal mixture, Chi-squared) and time quantiles (0.1, 0.25, 0.5, 0.75).

methods such as **cenROC** and **smoothROCtime** also perform well, but do not outperform **NPB**, particularly for more complex biomarker distributions like the normal mixture and chi-squared. Supplementary Figure 10 provides additional results for different sample sizes with a 50% censoring rate and a correlation of $\rho = -0.7$.

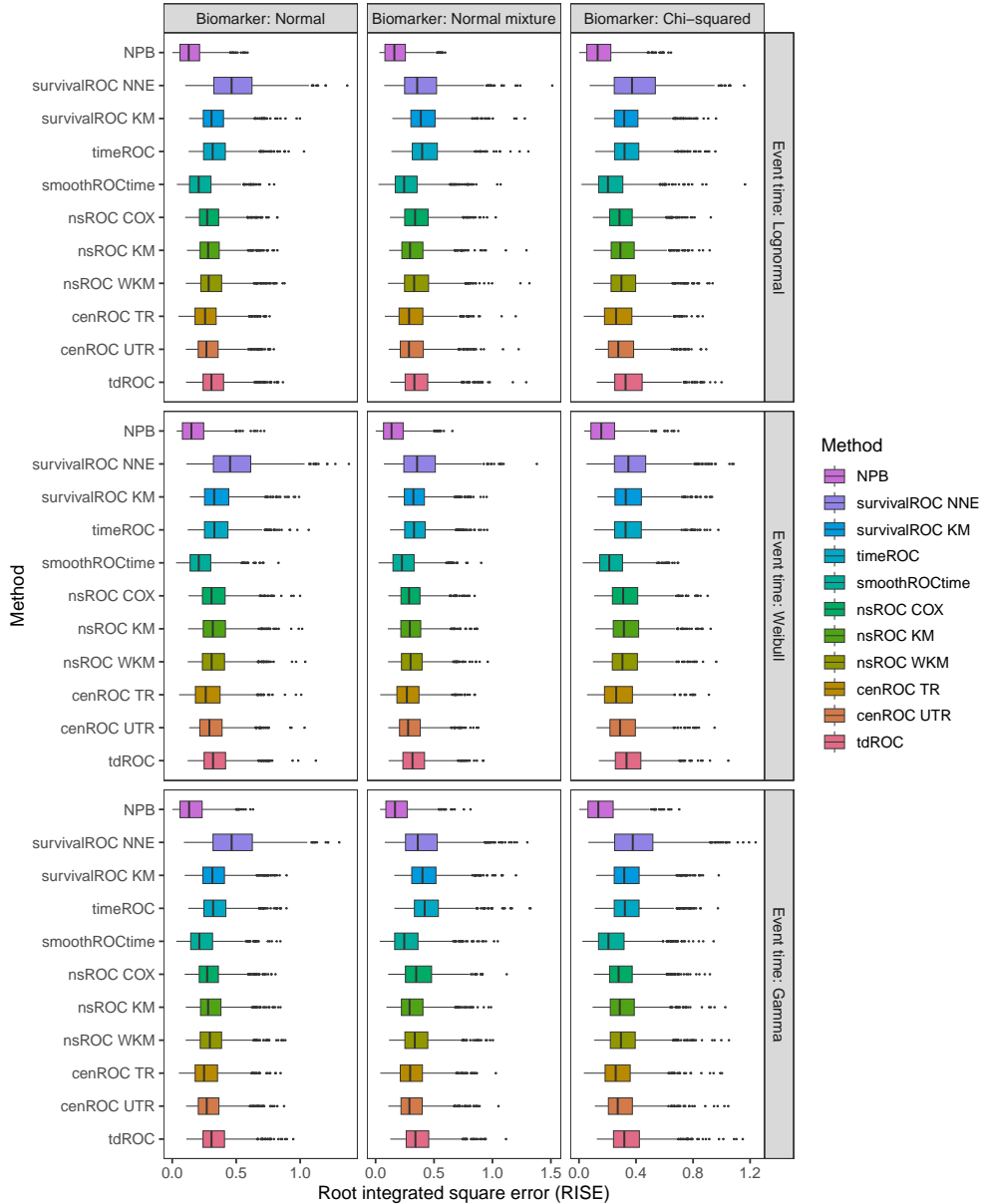


Figure 3: Distribution of root integrated squared errors (RISE) for unconditional ROC estimators at the median time quantile with a sample size of $N = 500$, event time distributions of $\{\text{Lognormal}, \text{Weibull}, \text{Gamma}\}$, 30% censoring rate and a correlation of $\rho = -0.5$ between transformed biomarker and event time distributions.

6.3. Conditional results

For the conditional case, we generated a continuous covariate from a standard uniform distribution $X \sim U(0, 1)$. To ensure consistency with the marginal distributions from the previously described unconditional data generating process and to incorporate the covariate shift on a standardized scale, we adjusted \mathbf{Z} to $(Z_1 + \gamma_Y X, Z_2 + \gamma_T X)$ where $\gamma_Y = 0.5$ and $\gamma_T = 3$. We then applied the standard normal CDF followed by the appropriate quantile function of the

marginal distribution.

We compare our NPB approach to the only existing method for time-dependent ROC analysis with covariates that has available code. The R package **CondTimeROC** implements a nonparametric kernel smoothing technique for one continuous covariate (Rodríguez-Álvarez *et al.* 2016). There are several estimators implemented in the package: smooth with bandwidth selected using a plug-in approach (Altman and Leger 1995) or data-driven (Li *et al.* 2013) and completely nonparametric. The package also implements the semiparametric technique of Song and Zhou (2008).

For the various methods, we evaluated the covariate-specific ROC curve $\text{ROC}_t(x)$ at different values of the covariate using functional boxplots, shown in Figure 4. These plots summarize the ROC functions over 1000 replications. The dashed line represents the median function, the grey area highlights the 50% central region and the blue curves are analogous to whiskers in a traditional boxplot. The red curve represents the ROC curve from the true data-generating process. To ensure comparable sensitivity and specificity calculations across methods, we varied t based on covariates so that each analysis included an equal number of uncensored observations. This adjustment was necessary for the nonparametric methods, which had high variance when only a few data points were available for estimation. The NPB model estimates are unbiased and show low variance. In contrast, the ROC estimates from the smoothing method appear sensitive to the choice of bandwidth, leading to bias in some cases. The nonparametric estimates are unbiased but show high variability, while the semiparametric estimates are biased, likely due to the violation of the proportional hazards assumption.

We also evaluated the performance of parameter estimates from our NPB model in the presence of multiple covariates. For this, we generated two continuous covariates from a standard uniform distribution and one binary covariate. Supplementary Figure 11 presents the bias of the parameter estimates under different sample sizes and censoring proportions. The likelihood-based inference procedures produced unbiased and efficient estimates. However, it is important to note that when the dependency structure changes or when the covariates include nonlinear terms, the estimates can become biased. The performance of the NPB under model misspecification is evaluated in Supplementary Material B.2.

7. Application to prognostic biomarkers in ALS

In this section, we apply our framework to data from our motivational study on prognostic biomarkers for ALS (Benatar *et al.* 2020). Serum NfL values in the current report were corrected for a 4-fold dilution factor that was inadvertently omitted in the previous publication. We apply the NPB model to determine the prognostic accuracy of baseline serum NfL concentration in predicting survival time in ALS. Our analysis begins with an unconditional model and we then incorporate baseline covariates to assess their impact on prognostic accuracy.

7.1. Unconditional NPB model

We estimated the unconditional NPB model to evaluate the prognostic accuracy of baseline neurofilament light (NfL) concentration for predicting survival time in patients with ALS. Supplementary Figure 15 displays the estimated joint density of the biomarker and event time, showing good agreement with the observed data. The model successfully captures the negative association between baseline NfL levels and survival time. Model diagnostics

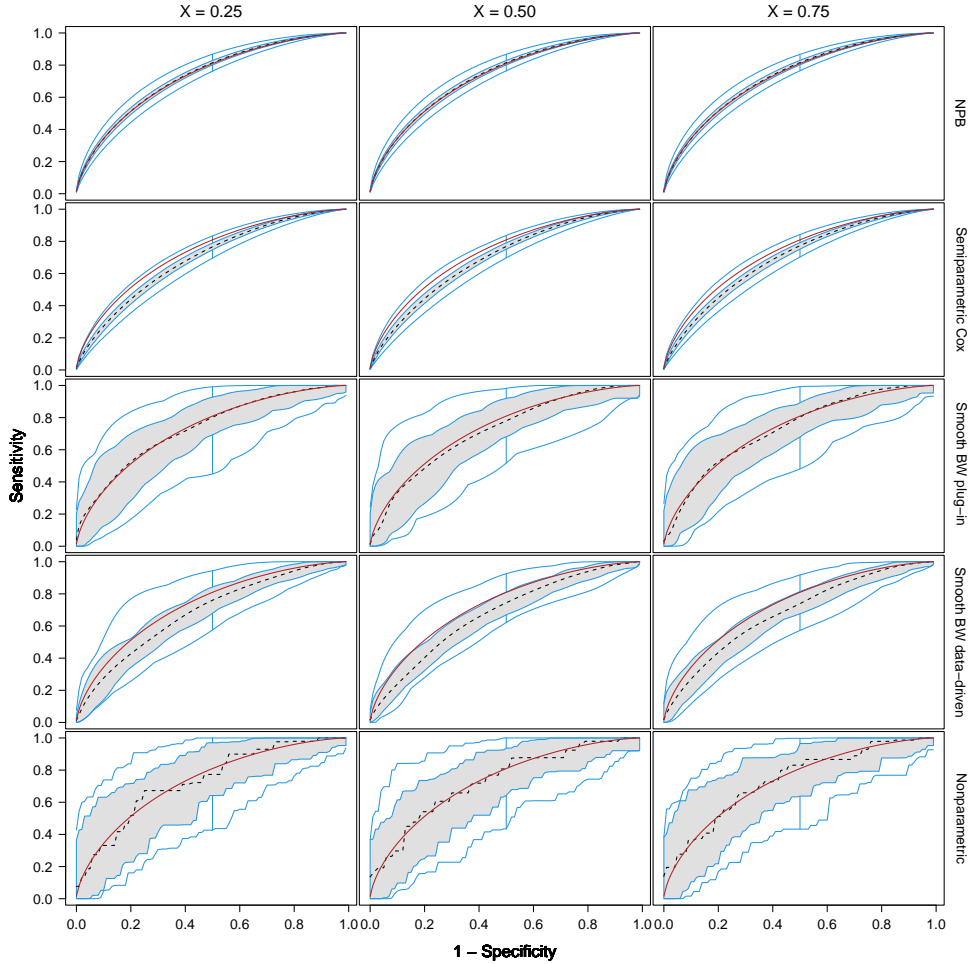


Figure 4: Functional boxplots for covariate-specific time dependent ROC curves at the median time quantile, with a sample size of $N = 500$, Weibull event time distribution, 30% censoring rate, and a correlation of $\rho = -0.5$ between transformed biomarker and event time distributions. The red line indicates the true covariate-specific ROC curve for each case.

using QQ plots of the PIT values (Supplementary Figure 13) revealed no evidence of major misspecification.

Using the fitted model, we derived the time-dependent ROC curve and associated summary measures, including the area under the curve (AUC), Youden index, optimal threshold, sensitivity and specificity. The optimal NfL threshold corresponds to the point at which the sum of sensitivity and specificity is maximized. Table 2 presents the estimated summary statistics along with their corresponding 95% confidence intervals. The results indicate that the prognostic utility of baseline NfL concentration decreases over longer prediction horizons

Access to the joint distribution allows us to estimate the survival time distribution for specific ranges of baseline NfL concentrations. NfL levels were categorized into tertiles (low, medium, high), as shown in Figure 5. The results depict an association between higher NfL levels and shorter survival times, with the highest tertile exhibiting the steepest decline in survival

Time (months)	AUC (95% CI)	Youden index (95% CI)	Optimal threshold (95% CI)	Sensitivity (95% CI)	Specificity (95% CI)
3	0.78 (0.70, 0.86)	0.42 (0.29, 0.55)	92.93 (77.82, 108.04)	0.73 (0.66, 0.80)	0.69 (0.63, 0.76)
6	0.75 (0.68, 0.83)	0.37 (0.26, 0.49)	84.85 (72.50, 97.19)	0.71 (0.65, 0.78)	0.66 (0.61, 0.71)
12	0.71 (0.65, 0.78)	0.31 (0.21, 0.41)	76.77 (65.71, 87.83)	0.66 (0.60, 0.72)	0.65 (0.60, 0.70)
24	0.70 (0.63, 0.76)	0.28 (0.19, 0.38)	64.65 (55.38, 73.92)	0.65 (0.60, 0.70)	0.63 (0.58, 0.68)

Table 2: Model-based summary statistics describing the prognostic accuracy of baseline serum NfL concentration for predicting survival at different time points. The table includes the AUC, Youden index, optimal threshold for NfL concentration, sensitivity and specificity at the optimal threshold, each presented with their corresponding 95% confidence intervals (CI) at 3, 6, 12, and 24 months.

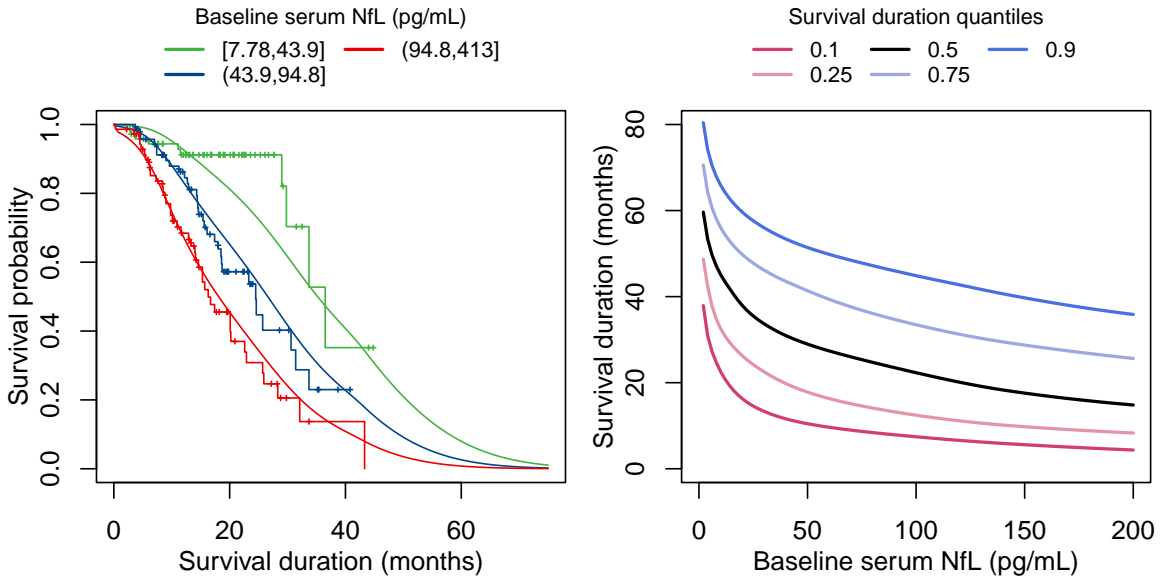


Figure 5: Left: Survival curves stratified by tertiles of baseline serum neurofilament light (NfL) concentration. Right: Survival time quantiles as a function of baseline serum NfL concentration.

probability. The model also provides estimates for median survival time and other quantiles, showing that higher NfL levels predict shorter survival times across all quantiles. Additionally, the rate of decline in the post-ALSFRS-R score is strongly associated with ALS survival. Individuals with higher NfL levels exhibit a more rapid decline in ALSFRS-R scores, as shown in Supplementary Figure 16.

7.2. Conditional NPB model

While the unconditional model provides an overall view of the relationship between NfL and survival, incorporating covariates allows us to account for confounding effects and assess how these factors influence the prognostic accuracy of NfL. We considered several baseline factors that could influence the prognostic accuracy of NfL for ALS.

The mean baseline age of patients was 60.1 years (SD 11.7). The cohort comprised 93 females (42.7%) and 125 males (57.3%). In terms of genetic characteristics, the C9orf72 repeat expansion was present in 24 participants (11.0%) and absent in 194 patients (89.0%). Site of symptom onset was bulbar only for 42 participants (19.3%), limb only for 154 (70.6%), and other regions or multi-region for 22 (10.0%). The median baseline ALS Functional Rating Scale – Revised (ALSFRS-R) score was 36.0 points (IQR 9.0). We also assessed the past (i.e. pre-baseline) rate of disease progression, defined by

$$\Delta\text{FRS} = \frac{48 - \text{ALSFRS-R}_{\text{baseline}}}{\text{Months from onset to baseline}},$$

where 48 is the maximum score on the ALSFRS-R. The average ΔFRS was 0.60 points per month (SD 0.47).

For ease of the following visualizations, we fixed continuous variables to their mean values and categorical variables to their modal values, unless otherwise specified. We fit the conditional NPB model with the marginal model for NfL specified as

$$h_Y(Y_i | \boldsymbol{\vartheta}) = \beta_{Y,1}\text{Age}_i + f\beta_{Y,2}\text{Sex}_i + \beta_{Y,3}\text{C9}_i + \beta_{Y,4}\Delta\text{FRS}_i + \beta_{Y,5}\text{ALSF}_i + \beta_{Y,6}\text{Site}_i + Z$$

where the baseline transformation function is given by $h_Y(y | \boldsymbol{\vartheta}) = \sum_{m=0}^6 \vartheta_{Y,m} b_m(\log(y))$ and $Z \sim N(0, 1)$. The survival time model includes the same set of covariates and the marginal transformation function for the survival time follows an analogous Bernstein polynomial form.

Supplementary Figure 17 displays the estimated baseline transformation functions for both NfL and survival time. These are nonlinear highlighting the need of having transformation functions for both margins. Supplementary Figure 14 displays the QQ plots of PIT values. These indicate a generally good fit, though there may be slight departures in the upper tail of the survival distribution, likely due to reduced data support at longer follow-up times.

The coefficients of the joint model are presented in Table 3. The unconditional correlation indicates whether there is a significant association between the biomarker and event time. If the confidence interval for this correlation includes zero, the biomarker likely lacks prognostic accuracy. For NfL, the unconditional correlation coefficient is relatively strong at -0.429 , with a 95% confidence interval of -0.283 to -0.547 , indicating a significant association with survival duration. The conditional correlation shows a reduction compared to the unconditional correlation, suggesting that some of the covariates account for a portion of the variation in survival duration.

Figure 6 shows the estimated joint distribution of baseline NfL concentration and survival time by the site of ALS onset. In both groups, higher baseline NfL concentrations are generally associated with shorter survival times. Patients with bulbar-onset ALS show lower survival times and higher NfL concentrations compared to those with limb-onset ALS. This aligns with previous research, which suggests that bulbar-onset ALS typically has a more aggressive disease progression (Zoccolella *et al.* 2008).

Figure 7 shows the estimated age-specific time-dependent ROC curves. The accuracy of baseline NfL in predicting survival declines as the time horizon increases. For any given time horizon, the prognostic accuracy of NfL decreases with increasing age. Further, age appears to have a greater impact when predicting early ALS prognosis compared to later stages of the disease.

The effect of different covariate combinations on prognostic accuracy varies, making it challenging to summarize these effects with a single model-based statistic or covariate-specific

Variable	NfL	Survival time
	Coefficient (95% CI)	
Unconditional correlation	−0.428 (−0.283, −0.547)	
Conditional correlation	−0.324 (−0.149, −0.471)	
Covariates β_i		
Age	0.020 (0.010, 0.031)	−0.021 (−0.036, −0.006)
Sex - Male	0.565 (0.290, 0.840)	0.142 (−0.239, 0.522)
C9orf72 - Positive	0.389 (−0.055, 0.833)	−0.541 (−1.076, −0.006)
Δ FRS	0.801 (0.467, 1.135)	−0.513 (−0.885, −0.142)
Baseline ALSFRS-R	0.000 (−0.021, 0.021)	0.035 (0.015, 0.054)
Site - Bulbar only	0.700 (0.284, 1.116)	−0.282 (−0.721, 0.157)
Site - Other	0.284 (−0.129, 0.697)	0.649 (−0.067, 1.366)

Table 3: Estimated coefficients of the nonparanormal prognostic biomarker model along with their corresponding 95% confidence intervals (CI).

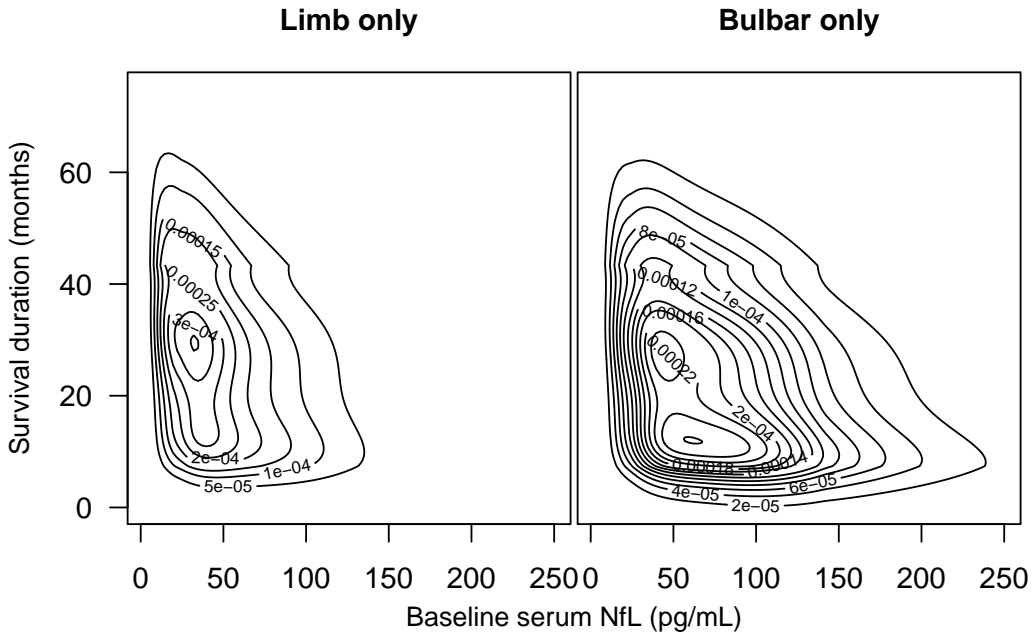


Figure 6: Bivariate density of baseline serum neurofilament light (NfL) concentration and survival time by the presence of the site of onset (limb only vs. bulbar only). The plot is based on fixed covariate values for a 60-year-old male with a negative C9orf72 status, a progression rate (Δ FRS) of 0.60 points/month and a baseline ALSFRS-R score of 35.

ROC curves. Figure 8 shows a spaghetti plot, where each line represents the time-dependent AUC for an individual patient's unique combination of covariates. The red line shows the smoothed average across all patients, while the blue line corresponds to the AUC from the unconditional model. Even after adjusting for covariates, the prognostic accuracy of base-

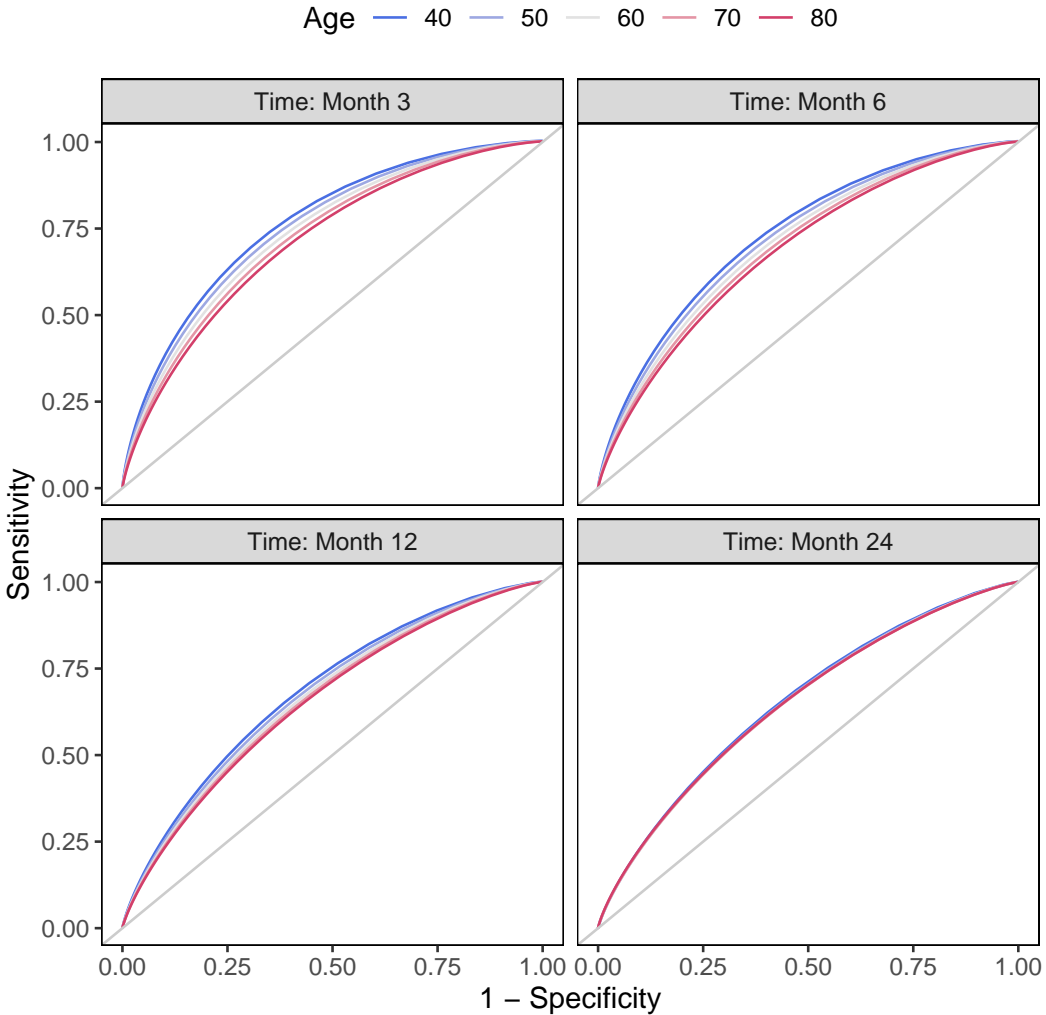


Figure 7: Covariate-specific time-dependent ROC curves by age and the presence of the C9orf72 repeat expansion for a female with a ΔFRS of 0.5. The plot is based on fixed covariate values for a male with a negative C9orf72 status, a progression rate (ΔFRS) of 0.60 points/month and a baseline ALSFRS-R score of 35.

line NfL declines over longer time horizons. However, incorporating covariates reduces the prognostic accuracy of NfL. Failing to account for these factors may lead to overly optimistic estimates.

Taken together, our findings emphasize the importance of covariate adjustment when evaluating prognostic biomarkers. The conditional NPB model revealed that the prognostic value of NfL is lower among patients with poorer prognostic factors such as older age, C9orf72-positive status, and higher ΔFRS . In contrast, factors such as sex, site of onset, and baseline ALSFRS-R showed limited influence on prognostic accuracy.

8. Discussion

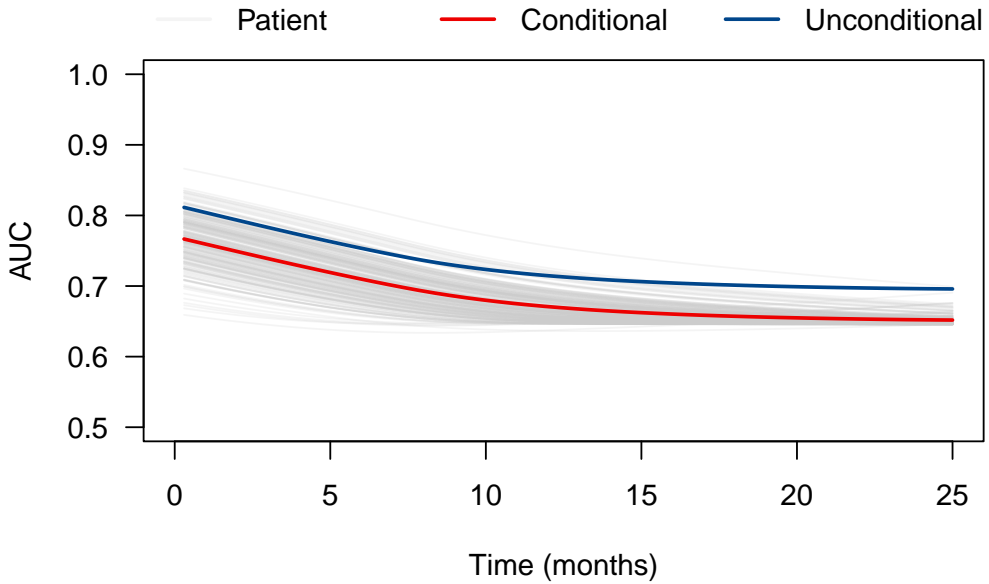


Figure 8: Spaghetti plot for patient-specific time-dependent AUCs (in gray), smoothed average across all patients (red) and unconditional (blue).

In this paper, we present a flexible statistical framework for evaluating the prognostic accuracy of biomarkers over time, while accounting for patient characteristics. We construct time-dependent ROC curves and summary indices using model-based covariate-specific sensitivity and specificity. The proposed NPB model accommodates a broad class of functional forms for the marginals and handles both right- and interval-censoring within a unified likelihood-based approach. Simulation studies demonstrate that the method performs well even in small to moderate sample sizes. Model calibration can be evaluated using the proposed PIT-based diagnostics, including QQ plots adapted to censored data and covariate-specific distributions.

One of the key advantages of our approach is its capacity to incorporate multiple covariates while retaining statistical efficiency. The parametric transformation models for the marginals yield near semiparametric-efficient estimators even in small samples (Hothorn 2024b), which translates to low-variance estimates of time-dependent AUC and other ROC-based measures, as shown in our simulations. By using a full-likelihood formulation rather than a two-stage or surrogate approach, we obtain closed-form score functions and enable valid likelihood-based inference, including confidence for all model parameters. The same framework also handles a wide range of data complexities, including detection limits, mixed outcome types and various forms of censoring without the need for combining different estimators to handle each setting individually.

Several areas warrant further investigation. As with any joint modeling framework, the validity of the results depends on the adequacy of the model assumptions. Our simulations show that while the NPB model performs well under correlation-driven dependence structures, it can yield biased results when the relationship between biomarker and event time is a direct

functional form (Supplementary Figure 12). To address this, we proposed a PIT-based diagnostic approach to assess the model calibration. These diagnostics are adapted for censored data and covariates, and showed no substantial misspecification in our ALS application. Also, although we focused on the Gaussian copula in the paper, the framework can be extended to alternative copula families and future work should explore such generalizations.

We chose a linear predictor for covariates to maintain simplicity. However, the framework is flexible and can be extended to accommodate non-linear effects through modifications to the marginal models. Additionally, while our method supports proportional hazards when appropriate, it is not limited to this assumption and allows for broader modeling choices. Covariate selection remains an important area for further development. Although model selection based on out-of-sample log-likelihoods is theoretically possible, it can be computationally demanding and impractical in smaller datasets. Rather than serving as a fully automated selection procedure, our framework is intended to support informed modeling decisions guided by clinical knowledge.

In practice, the choice of method for time-dependent ROC analysis involves a bias-variance trade-off. Fully nonparametric approaches are asymptotically unbiased and flexible but often suffer from high variance in small samples and typically cannot handle more than one covariate. In contrast, the proposed likelihood-based approach offers efficient estimation and covariate adjustment, but relies on model assumptions. Hybrid methods that strike a balance between flexibility and efficiency present an important area for future work.

We do not suggest our method as a default. In large datasets with minimal censoring and low-dimensional covariates, nonparametric or kernel-based approaches may suffice and require fewer assumptions. However, our method is particularly valuable in scenarios with limited sample sizes, complex censoring and covariate-driven heterogeneity in biomarker performance or when formal inference on model parameters is required.

As the number of candidate biomarkers continues to grow, so too does the need for robust statistical tools to evaluate their prognostic utility. The NPB framework provides a flexible and efficient solution for quantifying how biomarker performance varies across patient subgroups. This can support better risk stratification and can ultimately lead to more efficient clinical trials, by enabling more targeted inclusion criteria and reducing required sample sizes.

Computational details

We used **mvtnorm** (Genz *et al.* 2025, version 1.3.4) to sample from multivariate normal distributions, **pracma** (Borchers 2023, version 2.4.4) for numerical integration of ROC curves, and **qrng** (Hofert and Lemieux 2024, version 0.0.10) for random number generation.

To evaluate competitor methods in our simulation studies, we used the following R packages: **survivalROC** (Heagerty and Saha-Chaudhuri 2022, version 1.0.3.1) for nearest-neighbor and Kaplan-Meier estimations; **timeROC** (Blanche *et al.* 2013a, version 0.4) for inverse probability weighting; **smoothROCtime** (Diaz-Coto 2018, version 0.1.0) for bivariate kernel density estimation; **nsROC** (Fernandez 2018, version 1.1) for proportional hazards-based methods; **cen-ROC** (Beyene and El Ghouch 2023, version 2.0.0) for smoothed kernel methods; **tdROC** (Li *et al.* 2023, version 2.0) for nonparametric kernel smoothing weights. Each package was used to implement its respective method for estimating time-dependent ROC curves.

All computations were performed using R version 4.5.1 (R Core Team 2024).

A reference implementation of the nonparanormal prognostic biomarker model is available in the **tram** add-on package (Hothorn *et al.* 2025) to the R system for statistical computing. The simulation results presented in Sections 6 are available on <https://gitlab.com/asewak/npb>. The application to prognostic biomarkers in ALS in Section 7 can be reproduced by running the code from within R:

```
install.packages("tram")
library("tram")
demo("npb", package = "tram")
```

Acknowledgements

Torsten Hothorn received financial support from the Swiss National Science Foundation (grant number 200021_219384).

References

Altman N, Leger C (1995). “Bandwidth Selection for Kernel Distribution Function Estimation.” *Journal of Statistical Planning and Inference*, **46**(2), 195–214. [doi:10.1016/0378-3758\(94\)00102-2](https://doi.org/10.1016/0378-3758(94)00102-2).

Bansal A, Heagerty PJ (2019). “A Comparison of Landmark Methods and Time-Dependent ROC Methods to Evaluate the Time-Varying Performance of Prognostic Markers for Survival Outcomes.” *Diagnostic and Prognostic Research*, **3**, 1–13. [doi:10.1186/s41512-019-0057-6](https://doi.org/10.1186/s41512-019-0057-6).

Barratt S, Boyd S (2023). “Covariance Prediction via Convex Optimization.” *Optimization and Engineering*, **24**(3), 2045–2078. [doi:10.1007/s11081-022-09765-w](https://doi.org/10.1007/s11081-022-09765-w).

Benatar M, Macklin EA, Malaspina A, Rogers ML, Hornstein E, Lombardi V, Renfrey D, Shepheard S, Magen I, Cohen Y, Granit V, Statland JM, Heckmann JM, Rademakers R, McHutchison CA, Petrucci L, McMillan CT, Wuu J, CReATe Consortium PGB1 Study Investigators (2024). “Prognostic Clinical and Biological Markers for Amyotrophic Lateral Sclerosis Disease Progression: Validation and Implications for Clinical Trial Design and Analysis.” *eBioMedicine*, **108**, 105323. [doi:10.1016/j.ebiom.2024.105323](https://doi.org/10.1016/j.ebiom.2024.105323).

Benatar M, Wuu J, Turner MR (2023). “Neurofilament Light Chain in Drug Development for Amyotrophic Lateral Sclerosis: A Critical Appraisal.” *Brain*, **146**(7), 2711–2716. [doi:10.1093/brain/awac394](https://doi.org/10.1093/brain/awac394).

Benatar M, Zhang L, Wang L, Granit V, Statland J, Barohn R, Swenson A, Ravits J, Jackson C, Burns TM, Trivedi J, Pioro EP, Caress J, Katz J, McCauley JL, Rademakers R, Malaspina A, Ostrow LW, Wuu J, Hussain S, Cooley A, Li Y, Wallace M, Steele J, Hernandez JP, Medina J, Paredes ME, Manso A, Ravelo N, Levy W, Whitehead P, Zuchner S, Pasnoor M, Jawdat O, Jabari D, Farmakidis C, Glenn M, Dimachkie MM, Herbelin L, Tanui H, Anderson S, Walker M, Liu T, McCally A, Heim A, Currence M, Harness Y, Sieren J, Gibson E, Gutierrez G, Bussey D, Previte R, Kittrell P, Joshi A, Conger A, Hastings D, Caristo I, Marandi M, Carty S, Taylor JP, Wu G, Rampersaud E, Schule R, van Blitterswijk M (2020). “Validation of Serum Neurofilaments As Prognostic and Potential Pharmacodynamic Biomarkers for ALS.” *Neurology*, **95**(1), e59–e69. [doi:10.1212/wnl.0000000000009559](https://doi.org/10.1212/wnl.0000000000009559).

Beyene KM, Chen DG (2024). “Time-Dependent Receiver Operating Characteristic Curve Estimator for Correlated Right-Censored Time-To-Event Data.” *Statistical Methods in Medical Research*, **33**(1), 162–181. [doi:10.1177/09622802231220496](https://doi.org/10.1177/09622802231220496).

Beyene KM, El Ghouch A (2020). “Smoothed Time-Dependent Receiver Operating Characteristic Curve for Right Censored Survival Data.” *Statistics in Medicine*, **39**(24), 3373–3396. [doi:10.1002/sim.8671](https://doi.org/10.1002/sim.8671).

Beyene KM, El Ghouch A (2022). “Time-dependent ROC Curve Estimation for Interval-Censored Data.” *Biometrical Journal*, **64**(6), 1056–1074. [doi:10.1002/bimj.202000382](https://doi.org/10.1002/bimj.202000382).

Beyene KM, El Ghouch A (2023). *cenROC: Estimating Time-Dependent ROC Curve and AUC for Censored Data*. [doi:10.32614/CRAN.package.cenROC](https://doi.org/10.32614/CRAN.package.cenROC). R package version 2.0.0.

Blanche P, Dartigues JF, Jacqmin-Gadda H (2013a). “Estimating and Comparing Time-Dependent Areas under Receiver Operating Characteristic Curves for Censored Event Times with Competing Risks.” *Statistics in Medicine*, **32**(30), 5381–5397. [doi:10.1002/sim.5958](https://doi.org/10.1002/sim.5958).

Blanche P, Dartigues JF, Jacqmin-Gadda H (2013b). “Review and Comparison of ROC Curve Estimators for a Time-Dependent Outcome with Marker-Dependent Censoring.” *Biometrical Journal*, **55**(5), 687–704. [doi:10.1002/bimj.201200045](https://doi.org/10.1002/bimj.201200045).

Borchers HW (2023). *pracma: Practical Numerical Math Functions*. [doi:10.32614/CRAN.package.pracma](https://doi.org/10.32614/CRAN.package.pracma). R package version 2.4.4.

Cai T, Pepe MS, Zheng Y, Lumley T, Jenny NS (2006). “The Sensitivity and Specificity of Markers for Event Times.” *Biostatistics*, **7**(2), 182–197. [doi:10.1093/biostatistics/kxi047](https://doi.org/10.1093/biostatistics/kxi047).

Cox DR (1972). “Regression Models and Life-Tables.” *Journal of the Royal Statistical Society: Series B (Methodological)*, **34**(2), 187–202. [doi:10.1111/j.2517-6161.1972.tb00899.x](https://doi.org/10.1111/j.2517-6161.1972.tb00899.x).

Czado C, Van Keilegom I (2023). “Dependent Censoring Based on Parametric Copulas.” *Biometrika*, **110**(3), 721–738. [doi:10.1093/biomet/asac067](https://doi.org/10.1093/biomet/asac067).

Dawid AP (1984). “Present Position and Potential Developments: Some Personal Views Statistical Theory the Prequential Approach.” *Journal of the Royal Statistical Society: Series A (General)*, **147**(2), 278–290. [doi:10.2307/2981683](https://doi.org/10.2307/2981683).

Deresa NW, Van Keilegom I (2024). “Copula Based Cox Proportional Hazards Models for Dependent Censoring.” *Journal of the American Statistical Association*, **119**(546), 1044–1054. [doi:10.1080/01621459.2022.2161387](https://doi.org/10.1080/01621459.2022.2161387).

Dey R, Hanley JA, Saha-Chaudhuri P (2023). “Inference for Covariate-adjusted Time-dependent Prognostic Accuracy Measures.” *Statistics in Medicine*, **42**(23), 4082–4110. [doi:10.1002/sim.9848](https://doi.org/10.1002/sim.9848).

Diaz-Coto S (2018). *smoothROCtime: Smooth Time-Dependent ROC Curve Estimation*. [doi:10.32614/CRAN.package.smoothROCtime](https://doi.org/10.32614/CRAN.package.smoothROCtime). R package version 0.1.0.

Etzioni R, Pepe M, Longton G, Hu C, Goodman G (1999). “Incorporating the Time Dimension in Receiver Operating Characteristic Curves: A Case Study of Prostate Cancer.” *Medical Decision Making*, **19**(3), 242–251. [doi:10.1177/0272989x9901900303](https://doi.org/10.1177/0272989x9901900303).

Farouki RT (2012). “The Bernstein Polynomial Basis: A Centennial Retrospective.” *Computer Aided Geometric Design*, **29**(6), 379–419. [doi:10.1016/j.cagd.2012.03.001](https://doi.org/10.1016/j.cagd.2012.03.001).

Feldman EL, Goutman SA, Petri S, Mazzini L, Savelieff MG, Shaw PJ, Sobue G (2022). “Amyotrophic Lateral Sclerosis.” *The Lancet*, **400**(10360), 1363–1380. [doi:10.1016/s0140-6736\(22\)01272-7](https://doi.org/10.1016/s0140-6736(22)01272-7).

Fernandez SP (2018). *nsROC: Non-Standard ROC Curve Analysis*. [doi:10.32614/CRAN.package.nsROC](https://doi.org/10.32614/CRAN.package.nsROC). R package version 1.1.

Freidlin B, McShane LM, Korn EL (2010). “Randomized Clinical Trials with Biomarkers: Design Issues.” *Journal of the National Cancer Institute*, **102**(3), 152–160. [doi:10.1093/jnci/djp477](https://doi.org/10.1093/jnci/djp477).

Genz A (1992). “Numerical Computation of Multivariate Normal Probabilities.” *Journal of Computational and Graphical Statistics*, **1**(2), 141–149. [doi:10.2307/1390838](https://doi.org/10.2307/1390838).

Genz A, Bretz F, Miwa T, Mi X, Hothorn T (2025). *mvtnorm: Multivariate Normal and t Distributions*. [doi:10.32614/CRAN.package.mvtnorm](https://doi.org/10.32614/CRAN.package.mvtnorm). R package version 1.3-4.

Gneiting T, Balabdaoui F, Raftery AE (2007). “Probabilistic Forecasts, Calibration and Sharpness.” *Journal of the Royal Statistical Society Series B: Statistical Methodology*, **69**(2), 243–268. [doi:10.1111/j.1467-9868.2007.00587.x](https://doi.org/10.1111/j.1467-9868.2007.00587.x).

Harrell Jr FE (2015). “Ordinal Logistic Regression.” In *Regression Modeling Strategies*, pp. 311–325. Springer. [doi:10.1007/978-3-319-19425-7_13](https://doi.org/10.1007/978-3-319-19425-7_13).

Heagerty PJ, Lumley T, Pepe MS (2000). “Time-Dependent ROC Curves for Censored Survival Data and a Diagnostic Marker.” *Biometrics*, **56**(2), 337–344. [doi:10.1111/j.0006-341x.2000.00337.x](https://doi.org/10.1111/j.0006-341x.2000.00337.x).

Heagerty PJ, Saha-Chaudhuri P (2022). *survivalROC: Time-Dependent ROC Curve Estimation from Censored Survival Data*. [doi:10.32614/CRAN.package.survivalROC](https://doi.org/10.32614/CRAN.package.survivalROC). R package version 1.0.3.1.

Heagerty PJ, Zheng Y (2005). “Survival Model Predictive Accuracy and ROC Curves.” *Biometrics*, **61**(1), 92–105. [doi:10.1111/j.0006-341x.2005.030814.x](https://doi.org/10.1111/j.0006-341x.2005.030814.x).

Hofert M, Lemieux C (2024). *qrng: (Randomized) Quasi-Random Number Generators*. [doi:10.32614/CRAN.package.qrng](https://doi.org/10.32614/CRAN.package.qrng). R package version 0.0-10.

Hothorn T (2024a). *Multivariate Normal Log-likelihoods in the mvtnorm Package*. [doi:10.32614/CRAN.package.mvtnorm](https://doi.org/10.32614/CRAN.package.mvtnorm). R package vignette version 1.3-0.

Hothorn T (2024b). “On Nonparanormal Likelihoods.” [doi:10.48550/arXiv.2408.17346](https://doi.org/10.48550/arXiv.2408.17346). arXiv:2408.17346 [stat.ME].

Hothorn T, Möst L, Bühlmann P (2018). “Most Likely Transformations.” *Scandinavian Journal of Statistics*, **45**(1), 110–134. [doi:10.1111/sjos.12291](https://doi.org/10.1111/sjos.12291).

Hothorn T, Siegfried S, Kook L (2025). *tram: Transformation Models*. [doi:10.32614/CRAN.package.tram](https://doi.org/10.32614/CRAN.package.tram). R package version 1.2-3.

Janes H, Pepe MS (2008). “Adjusting for Covariates in Studies of Diagnostic, Screening, or Prognostic Markers: An Old Concept in a New Setting.” *American Journal of Epidemiology*, **168**(1), 89–97. [doi:10.1093/aje/kwn099](https://doi.org/10.1093/aje/kwn099).

Jiang X, Li W, Li R, Ning J (2024). “Addressing Subject Heterogeneity in Time-dependent Discrimination for Biomarker Evaluation.” *Statistics in Medicine*, **43**(7), 1341–1353. [doi:10.1002/sim.10024](https://doi.org/10.1002/sim.10024).

Kamarudin AN, Cox T, Kolamunnage-Dona R (2017). “Time-Dependent ROC Curve Analysis in Medical Research: Current Methods and Applications.” *BMC Medical Research Methodology*, **17**, 1–19. [doi:10.1186/s12874-017-0332-6](https://doi.org/10.1186/s12874-017-0332-6).

Kiernan MC, Vucic S, Talbot K, McDermott CJ, Hardiman O, Shefner JM, Al-Chalabi A, Huynh W, Cudkowicz M, Talman P, Van den Berg LH, Dharmadasa T, Wicks P, Reilly C, Turner MR (2021). “Improving Clinical Trial Outcomes in Amyotrophic Lateral Sclerosis.” *Nature Reviews Neurology*, **17**(2), 104–118. [doi:10.1038/s41582-020-00434-z](https://doi.org/10.1038/s41582-020-00434-z).

Klein N, Hothorn T, Barbanti L, Kneib T (2022). “Multivariate Conditional Transformation Models.” *Scandinavian Journal of Statistics*, **49**, 116–142. [doi:10.1111/sjos.12501](https://doi.org/10.1111/sjos.12501).

Klugman SA, Parsa R (1999). “Fitting bivariate loss distributions with copulas.” *Insurance: mathematics and economics*, **24**(1-2), 139–148. [doi:10.1016/S0167-6687\(98\)00039-0](https://doi.org/10.1016/S0167-6687(98)00039-0).

Koini M, Pirpamer L, Hofer E, Buchmann A, Pinter D, Ropele S, Enzinger C, Benkert P, Leppert D, Kuhle J, Schmidt R, Khalil M (2021). “Factors Influencing Serum Neurofilament Light Chain Levels in Normal Aging.” *Aging*, **13**(24), 25729. [doi:10.18632/aging.203790](https://doi.org/10.18632/aging.203790).

Lambert J, Chevret S (2016). “Summary Measure of Discrimination in Survival Models Based on Cumulative/dynamic Time-Dependent ROC Curves.” *Statistical Methods in Medical Research*, **25**(5), 2088–2102. [doi:10.1177/0962280213515571](https://doi.org/10.1177/0962280213515571).

Le Borgne F, Combescure C, Gillaizeau F, Giral M, Chapal M, Giraudeau B, Foucher Y (2018). “Standardized and weighted time-dependent receiver operating characteristic curves to evaluate the intrinsic prognostic capacities of a marker by taking into account confounding factors.” *Statistical Methods in Medical Research*, **27**(11), 3397–3410. [doi:10.1177/0962280217702416](https://doi.org/10.1177/0962280217702416).

Li L, Greene T, Hu B (2018). “A Simple Method to Estimate the Time-Dependent Receiver Operating Characteristic Curve and the Area under the Curve with Right Censored Data.” *Statistical Methods in Medical Research*, **27**(8), 2264–2278. [doi:10.1177/0962280216680239](https://doi.org/10.1177/0962280216680239).

Li Q, Lin J, Racine JS (2013). “Optimal Bandwidth Selection for Nonparametric Conditional Distribution and Quantile Functions.” *Journal of Business & Economic Statistics*, **31**(1), 57–65. [doi:10.1080/07350015.2012.738955](https://doi.org/10.1080/07350015.2012.738955).

Li S, Ning Y (2015). “Estimation of Covariate-Specific Time-Dependent ROC Curves in the Presence of Missing Biomarkers.” *Biometrics*, **71**(3), 666–676. [doi:10.1111/biom.12312](https://doi.org/10.1111/biom.12312).

Li X, Yin Z, Li L (2023). *tdROC: Nonparametric Estimation of Time-Dependent ROC, Brier Score, and Survival Difference from Right Censored Time-to-Event Data with or without Competing Risks*. [doi:10.32614/CRAN.package.tdROC](https://doi.org/10.32614/CRAN.package.tdROC). R package version 2.0.

Liu H, Lafferty J, Wasserman L (2009). “The Nonparanormal: Semiparametric Estimation of High Dimensional Undirected Graphs.” *Journal of Machine Learning Research*, **10**(80), 2295–2328. URL <http://jmlr.org/papers/v10/liu09a.html>.

Lu CH, Macdonald-Wallis C, Gray E, Pearce N, Petzold A, Norgren N, Giovannoni G, Fratta P, Sidle K, Fish M, Orrell R, Howard R, Talbot K, Greensmith L, Kuhle J, Turner MR,

Malaspina A (2015). “Neurofilament Light Chain: A Prognostic Biomarker in Amyotrophic Lateral Sclerosis.” *Neurology*, **84**(22), 2247–2257. [doi:10.1212/WNL.0000000000001642](https://doi.org/10.1212/WNL.0000000000001642).

Martínez-Camblor P, Pardo-Fernández JC (2018). “Smooth Time-Dependent Receiver Operating Characteristic Curve Estimators.” *Statistical Methods in Medical Research*, **27**(3), 651–674. [doi:10.1177/0962280217740786](https://doi.org/10.1177/0962280217740786).

Pepe MS (1997). “A Regression Modelling Framework for Receiver Operating Characteristic Curves in Medical Diagnostic Testing.” *Biometrika*, **84**(3), 595–608. [doi:10.1093/biomet/84.3.595](https://doi.org/10.1093/biomet/84.3.595).

Pepe MS, Janes H, Longton G, Leisenring W, Newcomb P (2004). “Limitations of the Odds Ratio in Gauging the Performance of a Diagnostic, Prognostic, or Screening Marker.” *American Journal of Epidemiology*, **159**(9), 882–890. [doi:10.1093/aje/kwh101](https://doi.org/10.1093/aje/kwh101).

Pérez-Fernández S, Martínez-Camblor P, Filzmoser P, Corral N (2018). “nsROC: An R package for Non-Standard ROC Curve Analysis.” *The R Journal*, **10**(2), 55–77. [doi:10.32614/RJ-2018-043](https://doi.org/10.32614/RJ-2018-043).

R Core Team (2024). *R: A Language and Environment for Statistical Computing*. R Foundation for Statistical Computing, Vienna, Austria. URL <https://www.R-project.org/>.

Rodríguez-Álvarez MX, Meira-Machado L, Abu-Assi E, Raposeiras-Roubín S (2016). “Non-parametric Estimation of Time-Dependent ROC Curves Conditional on a Continuous Covariate.” *Statistics in Medicine*, **35**(7), 1090–1102. [doi:10.1002/sim.6769](https://doi.org/10.1002/sim.6769).

Rosenblatt M (1952). “Remarks on a Multivariate Transformation.” *The Annals of Mathematical Statistics*, **23**(3), 470–472. [doi:10.1214/aoms/1177729394](https://doi.org/10.1214/aoms/1177729394).

Sewak A, Hothorn T (2023). “Estimating Transformations for Evaluating Diagnostic Tests with Covariate Adjustment.” *Statistical Methods in Medical Research*, **32**(7), 1403–1419. [doi:10.1177/09622802231176030](https://doi.org/10.1177/09622802231176030).

Slate EH, Turnbull BW (2000). “Statistical Models for Longitudinal Biomarkers of Disease Onset.” *Statistics in Medicine*, **19**(4), 617–637. [doi:10.1002/\(sici\)1097-0258\(20000229\)19:4<617::aid-sim360>3.0.co;2-r](https://doi.org/10.1002/(sici)1097-0258(20000229)19:4<617::aid-sim360>3.0.co;2-r).

Song X, Zhou XH (2008). “A Semiparametric Approach for the Covariate Specific ROC Curve with Survival Outcome.” *Statistica Sinica*, **18**(3), 947–965.

Stensrud MJ, Hernà MA (2025). “Invited Commentary: Why Use Methods That Require Proportional Hazards?” *American Journal of Epidemiology*, p. kwa361. [doi:10.1093/aje/kwa361](https://doi.org/10.1093/aje/kwa361).

Taga A, Maragakis NJ (2018). “Current and Emerging ALS Biomarkers: Utility and Potential in Clinical Trials.” *Expert Review of Neurotherapeutics*, **18**(11), 871–886. [doi:10.1080/14737175.2018.1530987](https://doi.org/10.1080/14737175.2018.1530987).

Yu D, Hwang WT (2019). “Optimal Cutoffs for Continuous Biomarkers for Survival Data under Competing Risks.” *Communications in Statistics-Simulation and Computation*, **48**(5), 1330–1345. [doi:10.1080/03610918.2017.1410713](https://doi.org/10.1080/03610918.2017.1410713).

Zoccolella S, Beghi E, Palagano G, Fraddosio A, Guerra V, Samarelli V, Lepore V, Simone IL, Lamberti P, Serlenga L, Logroscino G, for the SLAP Registry (2008). “Analysis of Survival and Prognostic Factors in Amyotrophic Lateral Sclerosis: A Population Based Study.” *Journal of Neurology, Neurosurgery & Psychiatry*, **79**(1), 33–37. [doi:10.1136/jnnp.2007.118018](https://doi.org/10.1136/jnnp.2007.118018).

A. Alternative ROC curve definitions

The NPB framework introduces an approach to time-dependent ROC analysis by modeling the joint distribution of the biomarker and event time conditional on covariates. This strategy allows for derivation of various ROC curve types, including incident-dynamic and incident-static, as well as associated summary indices such as the AUC and Youden Index. Unlike many existing methods, which are tailored to specific definitions of sensitivity or specificity, the NPB framework provides a way to derive all forms of time-dependent ROC curves.

A.1. Incident-dynamic

The *incident* sensitivity is the probability that a subject's biomarker value exceeds a threshold c at the exact time they experience the event

$$\text{Se}_t^{\mathbb{I}}(c \mid \mathbf{x}) = \mathbb{P}(Y > c \mid T = t, \mathbf{X} = \mathbf{x})$$

In this definition, cases are defined as subjects experiencing the event at time t , while subjects who experienced the event before t are excluded from the calculation. This leads to the *incident-dynamic* ROC curve, which evaluates the biomarker's ability to distinguish between subjects experiencing the event at $T = t$ and those who have not yet experienced it. This measure is particularly valuable for guiding treatment decisions at multiple time points.

Under the NPB framework, where the conditional distribution of the biomarker given event time is normal, incident sensitivity has a closed-form expression

$$\begin{aligned} \text{Se}_t^{\mathbb{I}}(c \mid \mathbf{x}) &= \Phi\left(\frac{\rho h_T(t \mid \mathbf{x}) - h_Y(c \mid \mathbf{x})}{\sqrt{1 - \rho^2}}\right) \\ &= \Phi\left(\frac{\mathbf{x}^\top \boldsymbol{\beta}_Y + \rho(h_T(t) - \mathbf{x}^\top \boldsymbol{\beta}_T) - h_Y(c)}{\sqrt{1 - \rho^2}}\right). \end{aligned}$$

The second form assumes linear transformation models for the marginal distributions of the biomarker and event time, as introduced in Section 4. Alternative marginal models can also be incorporated as discussed in Section 5. Note that in this setup incident sensitivity involves only the evaluation of a univariate distribution function.

A.2. Incident-static

Static sensitivity is particularly useful for comparing incident cases to control subjects who are long-term survivors, i.e., those who remain event-free throughout a fixed follow-up period $(0, t^*)$ (Etzioni *et al.* 1999). It is defined as

$$\text{Sp}^{\bar{\mathbb{D}}}(c \mid \mathbf{x}) = \mathbb{P}(Y \leq c \mid T > t^*, \mathbf{X} = \mathbf{x})$$

which leads to the *incident-static* ROC curve. Under the NPB framework, the joint model for the biomarker and event time remains the same as for the dynamic specificity case described in the main text. The key difference lies in the fact that $\text{Sp}^{\bar{\mathbb{D}}}$ is no longer dependent on the value of t . Instead it focuses on a fixed follow-up time t^* which is prespecified to a value which is considered a long enough time to observe the event of interest. The dependence on t is then restricted to the incident sensitivity component.

B. Additional simulation results

B.1. Simulations with different settings

This section presents additional simulations assessing the NPB framework. We use different event time distributions, sample sizes and censoring rates.

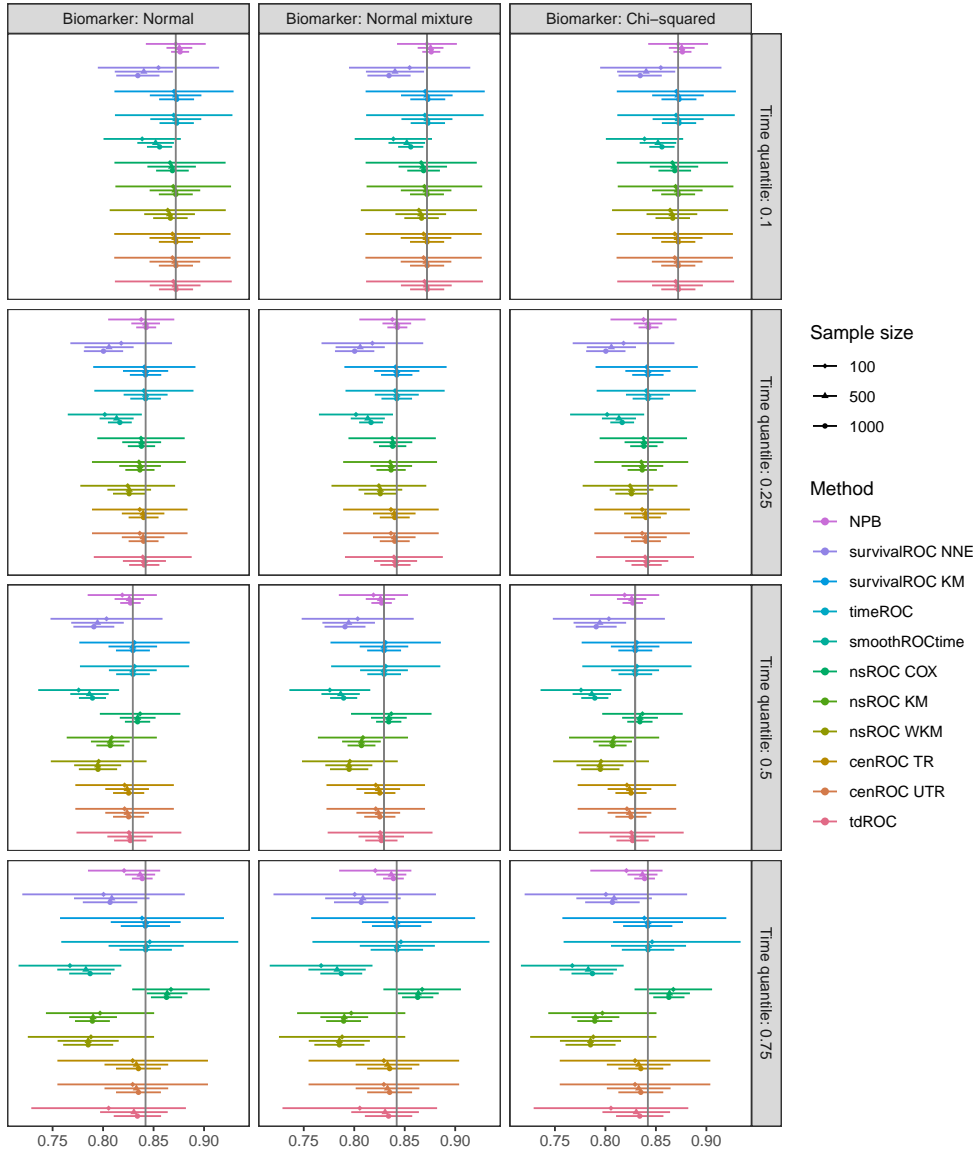


Figure 9: Mean and standard deviation of the unconditional AUC for each method with sample sizes of $N = \{100, 500, 1000\}$, Lognormal event time distribution, 50% censoring rate and a correlation of $\rho = -0.7$ between transformed biomarker and event time distributions. The evaluation is across different biomarker distributions (Normal, Normal mixture, Chi-squared) and time quantiles (0.1, 0.25, 0.5, 0.75).

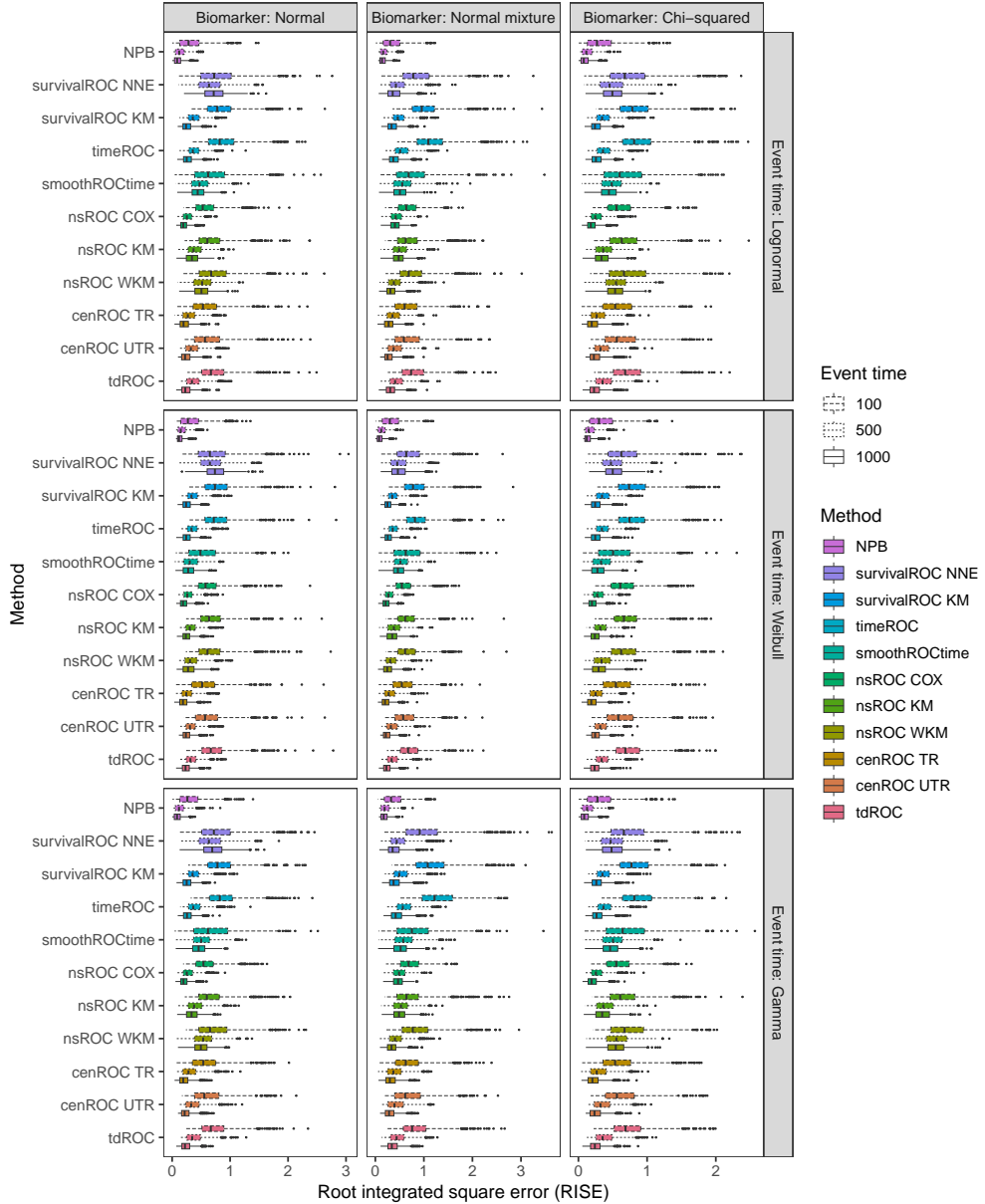


Figure 10: Distribution of root integrated squared errors (RISE) for unconditional ROC estimators at the median time quantile with sample sizes of $N \in \{100, 500, 1000\}$, event time distributions of $\{\text{Lognormal}, \text{Weibull}, \text{Gamma}\}$, 50% censoring rate and a correlation of $\rho = -0.7$ between transformed biomarker and event time distributions.

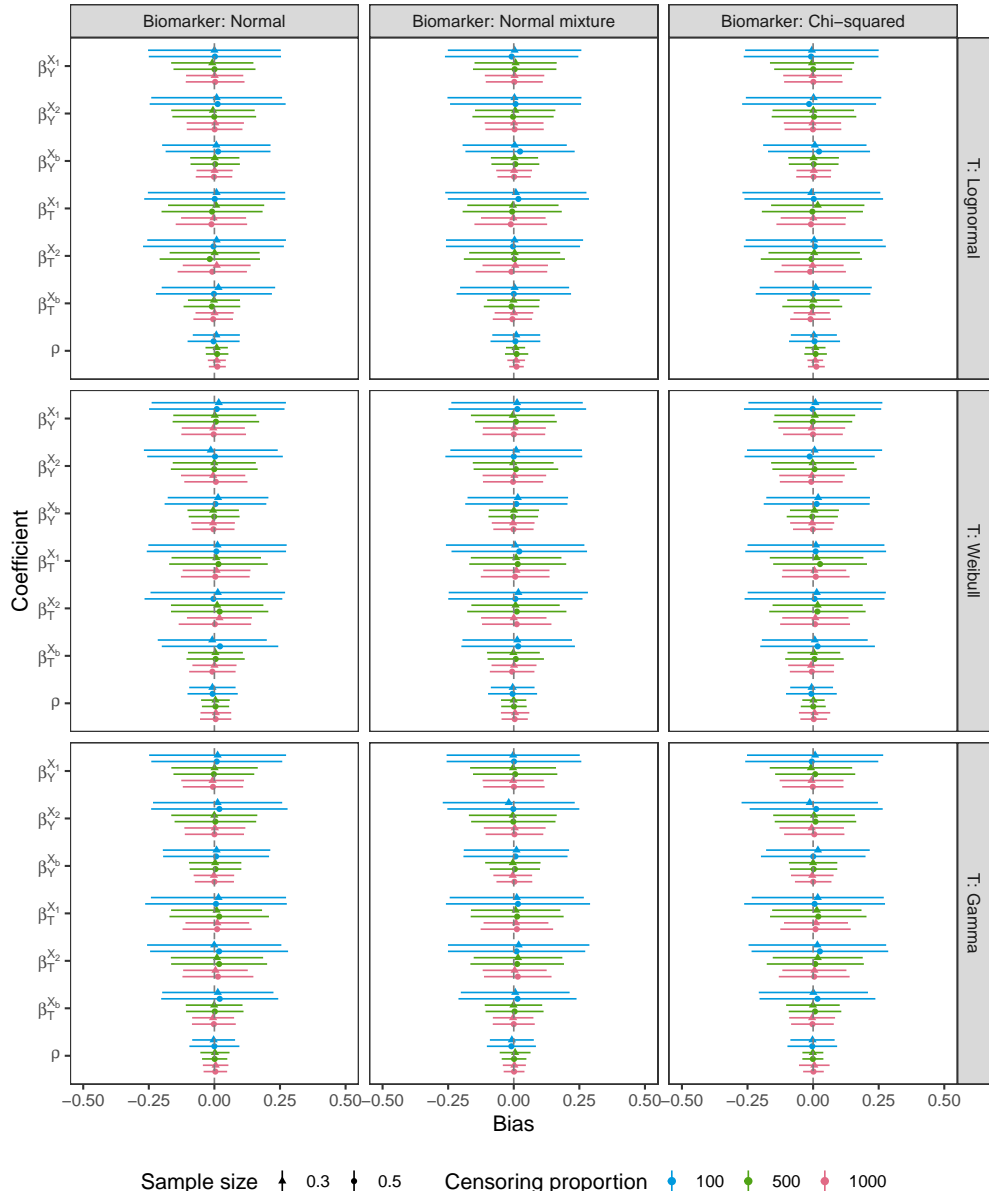


Figure 11: Mean and standard deviation of bias for coefficients for the NPB method with sample sizes of $N \in \{100, 500, 1000\}$, censoring rates of 30% and 50%, and a correlation of $\rho = -0.5$. Results are presented for varying biomarker distributions {Normal, Normal mixture, Chi-squared} and event time distributions {Lognormal, Weibull, Gamma}.

B.2. Simulations with dependence misspecification

We investigated how the NPB model performs when there is a misspecification of the dependence structure. For this, we considered an alternative DGP proposed by [Rodríguez-Álvarez et al. \(2016\)](#). In this setting the true relationship between the biomarker and event time deviates from the assumed copula-based dependence structure.

The covariate \mathbf{X} is generated from a normal distribution with mean 1 and variance 1, i.e., $\mathbf{X} \sim N(1, 1)$. The biomarker Y is then generated from a conditional normal distribution with mean $X = x$ and variance 1, i.e., $Y \sim N(x, 1)$. Finally, the survival time T is generated from a proportional hazards Weibull model, conditional on the biomarker and covariate. This corresponds to an accelerated failure time (AFT) model

$$\log(T) = y + 0.5x + Z,$$

where Z follows a minimum extreme value distribution.

To assess performance, we generated 1000 replications, with each dataset consisting of 500 observations with a censoring rate of 30%. We evaluated the covariate-specific cumulative-dynamic time-dependent ROC curves $ROC_t^{C/D}(x)$ 25th, 50th, and 75th percentiles of the covariate. Figure 12 displays functional boxplots of the results and compares the different covariate-specific time-dependent ROC curve methods for a single time point of 1.5.

The NPB model shows low bias for low quantiles of X . However, the bias increases across higher quantiles. The proportional hazards-based semiparametric method of [Song and Zhou \(2008\)](#) outperformed other methods, since it correctly aligns with the true DGP. The nonparametric kernel-based approach was largely unbiased across quantiles but exhibited higher variability.

These results suggest that while the NPB model effectively captures correlation-driven dependencies between biomarkers and event times, it struggles when the dependence follows a direct functional form. That is, when T is assumed to be a function of Y and X . This highlights a fundamental bias-variance trade-off for method selection. Model-based approaches tend to provide low-variance, unbiased estimates when correctly specified but can introduce bias when the true DGP differs from the assumed model. In contrast, fully nonparametric methods are asymptotically unbiased but often suffer from high variability in finite samples, making estimation less stable. Additionally, nonparametric approaches have problems in incorporating multiple covariates. Ultimately, the choice of method depends on the specific application and the needs of the target audience.

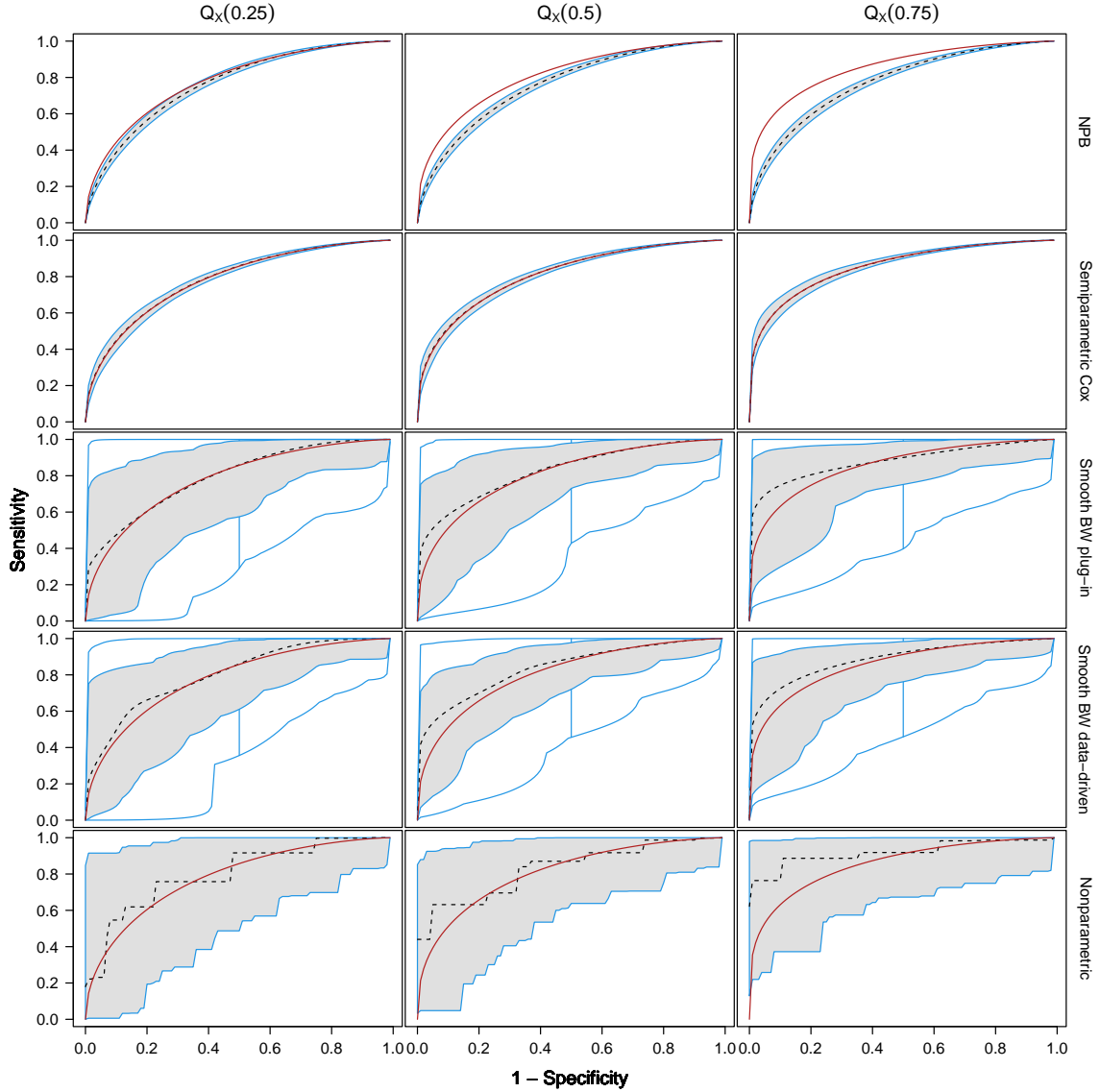


Figure 12: Functional boxplots for covariate-specific time dependent ROC curves at the median time quantile, with a sample size of $N = 500$, Weibull event time distribution, 30% censoring rate, and a correlation of $\rho = -0.5$ between transformed biomarker and event time distributions. The red line indicates the true covariate-specific ROC curve for each case.

C. Additional application results

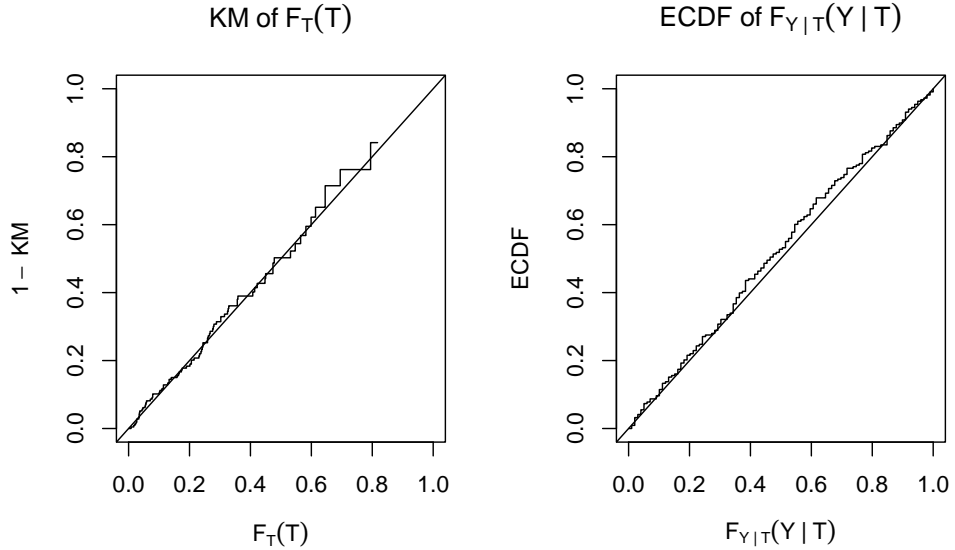


Figure 13: QQ-PIT diagnostic plots for assessing model calibration without covariates. Left: Kaplan–Meier estimate of PIT values for survival time. Right: ECDF of conditional PIT values for the biomarker, accounting for right censoring.

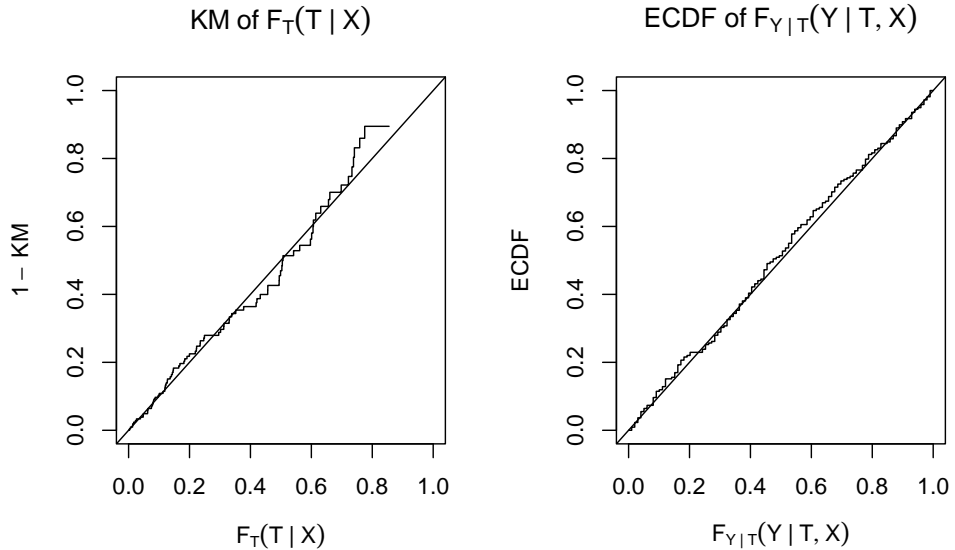


Figure 14: QQ-PIT diagnostic plots for assessing model calibration with covariates. Left: Kaplan–Meier estimate of PIT values for survival time given covariates. Right: ECDF of conditional PIT values for the biomarker, adjusted for covariates and right censoring.

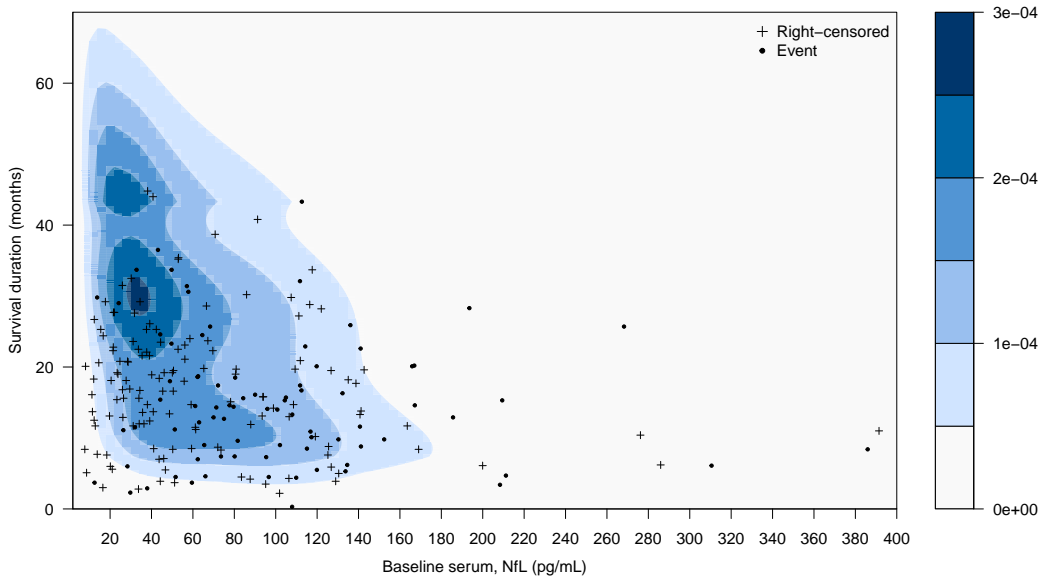


Figure 15: Estimated bivariate density of baseline serum neurofilament light (NfL) concentration (pg/mL) and survival time (in months since baseline) overlaid with observed data. Right censored subjects are indicated with “+” and subjects who reached the endpoint are marked by “•”.

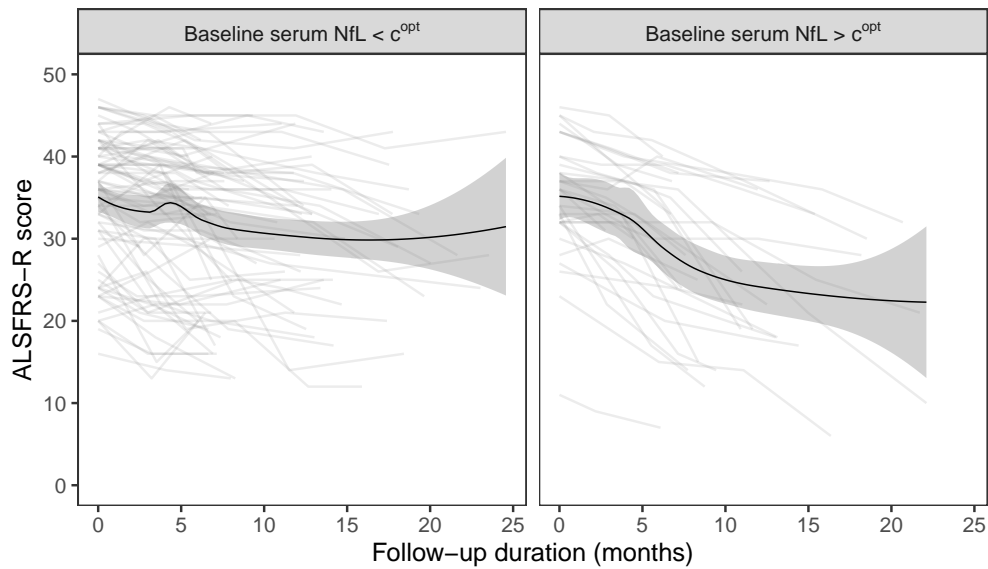


Figure 16: Spaghetti plot of ALSFRS-R scores over follow-up stratified by the optimal baseline serum neurofilament light concentration threshold for predicting 12-month survival.

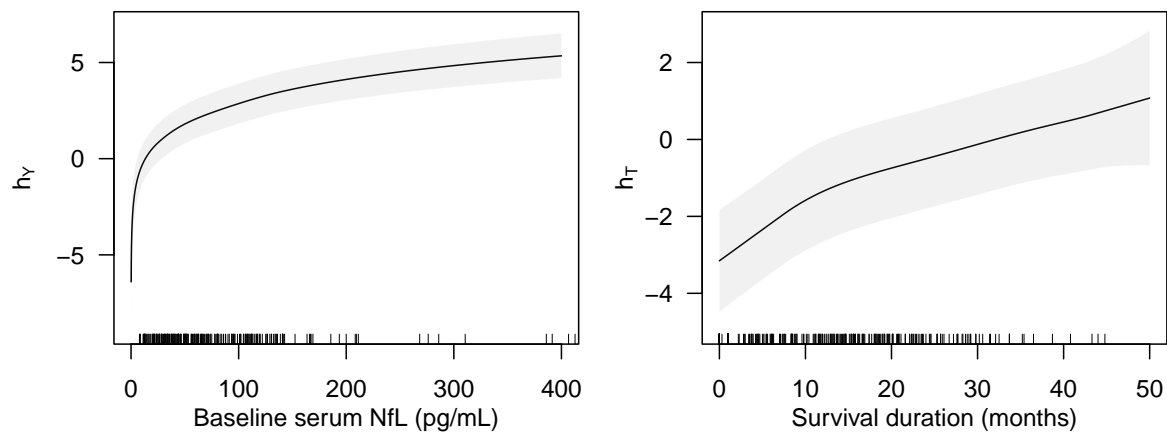


Figure 17: Estimated baseline transformation functions for baseline serum neurofilament light (NFL) concentration $h_Y(y | \hat{\vartheta}_Y)$ and survival time $h_T(t | \hat{\vartheta}_T)$.

Affiliation:

Ainesh Sewak
Department of Clinical Research
Universität Bern
Mittelstrasse 43, CH-3010 Bern, Switzerland
Email: Ainesh.Sewak@unibe.ch

Vanda Inácio
School of Mathematics
University of Edinburgh
Peter Guthrie Tait Road, EH9 3FD Edinburgh, United Kingdom
Email: Vanda.Inacio@ed.ac.uk

Joanne Wuu, Michael Benatar
Department of Neurology
University of Miami Miller School of Medicine
1120 NW 14th Street, Suite 1300, Miami, FL, 33136, United States
Email: MBenatar@med.miami.edu, JWuu@med.miami.edu

Torsten Hothorn
Institut für Epidemiologie, Biostatistik und Prävention
Universität Zürich
Hirschengraben 84, CH-8001 Zürich, Switzerland
Email: Torsten.Hothorn@R-project.org